A GEOLOGICAL APPROACH TO MODELING THE MOVEMENT OF GROUND WATER IN THE SHALLOW AQUIFER IN THE VICINITY OF THE BURTON RECHARGE AREA, BEAUFORT, SOUTH CAROLINA: PHASE 1

by

Michael G. Waddell

Earth Sciences and Resources Institute, University of South Carolina

[ESRI Technical Report 88-0015]

Prepared in cooperation with the

South Carolina Water Resources Commission

and the

South Carolina Coastal Council

STATE OF SOUTH CAROLINA

WATER RESOURCES COMMISSION

REPORT NUMBER 165

1989

STATE
OF
SOUTH CAROLINA

The Honorable Carroll A. Campbell, *Governor*

SOUTH CAROLINA WATER RESOURCES COMMISSION

Appointed Members

Mr. Erick B. Ficken, *Chairman*

Mr. Lynn H. Youmans, Jr., *Vice-Chairman*

Agriculture

Mr. Lynn H.Youmans, Jr. .... Furman
Mr. Lewis Walker .... Sumter
Mr. Ben M. Gramling, III .... Gramling

Industry

Mr. Floyd E. Williams .... Fort Mill
Mr. Fred Winslow .... Hartsville
Mr. Dan E. Jones .... Columbia

Municipalities

Mr. Tom W. Dunaway, III .... Anderson
Mayor Elsie Rast Stuart .... Pelion
Mr. Erick B. Ficken .... Myrtle Beach

Saltwater

Mr. Whitemarsh S. Smith .... Charleston

Ex Officio Members and Designees

Mr. D. Leslie Tindal
Commissioner
S.C. Department of Agriculture
Desig: Mr. David L. Tompkins

Mr. Michael D. Jarrett, Commissioner
S.C. Department of Health and
Environmental Control
Desig: Mr. R. Lewis Shaw

Mr. Boris Hurlbutt
Chairman
S.C. Forestry Commission
Desig: Mr. Robert J. Gould

Mr. Marion Burnside
Chairman
S.C. Wildlife & Marine
Resources Department
Desig: Mr. Larry D. Cartee

The Honorable L. Edward Bennett
Chairman
S.C. House Agriculture and
Natural Resources Committee
Desig: The Honorable John J. Snow, Jr.

Mr. Glenn C. Alexander
Chairman
S.C. Land Resources
Conservation Commission
Desig: Mr. Cary D. Chamblee

Mr. Richard E. Greer
Chairman
S.C. Development Board
Desig: Mr. O'Neal Laird

Dr. A. Max Lennon
President
Clemson University
Desig: Dr. Paul B. Zielinski

Mr. Joe G. Rideoutte
Commissioner
S.C. Department of Highways
and Public Transportation
Desig: Mr. Robert B. Ferrell

The Honorable John C. Land
Chairman
S.C. Senate Agriculture and
Natural Resources Committee
Desig: vacant

Staff

Alfred H. Vang, Executive Director
Hank W. Stallworth, Deputy Director
Camille Ransom, III, Director, Geology-Hydrology Division
A. Drennan Park, Regional Hydrologist, Beaufort

CONTENTS

	Page
Abstract	1
Introduction	1
Geologic setting	1
Structure	1
Tertiary stratigraphy	4
Eocene Series	4
Miocene Series	4
Pliocene to Holocene Series	4
Methodology	4
Description of geologic sections	11
Section A-A'	11
Section B-B'	14
Section C-C'	14
Section D-D'	15
Section E-E'	15
Section F-F'	16
Section G-G'	16
Section H-H'	16
Section I-I'	17
Isoresistivity contour maps	17
Deposition in the Burton recharge area	17
Depositional history	17
Depositional model	20
Effect of depositional environment on ground water movement	20
Conclusions	22
Acknowledgments	22
References cited	22

ILLUSTRATIONS

Figure		Page
1	Location of Port Royal Island and the Burton recharge area	2
2	Structural map of the top of the Ocala Formation	3
3	Generalized stratigraphic column and gamma-ray log response of the sediments of the shallow aquifer, the confining bed, and the upper unit of the Ocala Limestone	5
4	Schematic diagram showing the basic concept of resistivity measurements, path of current flow, and equipotential lines	6
5	Schematic diagram showing that the greater the electrode separation the greater the depth of investigation	7
6	Schematic diagram showing the electrode configuration for the Schlumberger Array	8
7A	Diagram showing the field resistivity values with a synthetic curve developed from the forward model, and the true resistivity values also derived from the forward model	10
7B	Diagram showing the forward resistivity model after a series of inversions	10
8	Schematic diagram showing the principle of seismic refraction, the path of the direct waves, and refracted seismic waves in a two-layered model	11
9	Locations of the vertical electrical soundings (VES), seismic-refraction stations, wells, and geologic sections	13
10	Contour map of apparent-resistivity values in the vinicity of the Burton recharge area	18
11	Contour map of true-resistivity values in the vinicity of the Burton recharge area	19
12	Stucture-contour map of the top of the Ocala Limestone in the vinicity of the Burton recharge area	21

TABLES

Table		Page
1	Resistivity field data	9
2	Resistivity values and layers after forward modeling	9
3	Seismic refraction velocities and interpretations	12

PLATES

Plate 1. Geologic sections A through C
Plate 2. Geologic sections D through F
Plate 3. Geologic sections G through I

A GEOLOGICAL APPROACH TO MODELING THE MOVEMENT OF GROUND WATER IN THE SHALLOW AQUIFER IN THE VICINITY OF THE BURTON RECHARGE AREA, BEAUFORT, SOUTH CAROLINA: PHASE 1

Michael G. Waddell

ABSTRACT

The Burton recharge area, located on Port Royal Island in Beaufort County, S.C., is the largest, and possibly the only, major recharge area for the Floridan aquifer on Port Royal Island. The amount of recharge is dependent upon several factors; one of the most important is the presence or absence of the confining unit separating the shallow unconfined aquifer from the deeper artesian aquifer, another is the textural characteristics of the overlying sediments. The present geologic study indicates that these factors are controlled by the depositional history of the shallow aquifer. Using surface geophysical methods (DC resistivity and multichannel seismic refraction) as the principal mapping tools, and available well and borehole data as a control, a depositional model was developed for the shallow aquifer in order to understand the movement of ground water in that aquifer.

During the Pleistocene, the area that is now the Burton recharge area was inundated by numerous marine transgressions and regressions. The area appears to have been a sand-dominated back barrier or lagoon environment during one regression. Tidal channels meandered throughout the back barrier system and appear to have eroded the Hawthorn Formation, allowing tidal channel sand to be deposited directly on the limestone. The channel deposits also controlled the textural characteristics of the sand. Where channeling occurred, the sand generally is well sorted and very fine gained with little or no clay and silt. The sand also generally coarsens downward to the limestone, providing an excellent pathway for water migration from the land surface to the limestone aquifer.

INTRODUCTION

The Burton recharge area, located on Port Royal Island in Beaufort County, S.C., is the largest, and possibly the only, major recharge area for the Floridan aquifer on Port Royal Island (Fig. 1). Any prospect of developing a ground-water flow model for the area depends upon determining its areal extent — the objective of this two-phase study.

The objective of Phase One is to develop a predictive geologic model for the shallower aquifer in the vicinity of the Burton recharge area and to determine the areal extent of recharge — that is, the presence or absence of a confining unit separating it from the deeper limestone (Floridan) aquifer.

A secondary objective of Phase One is to use different surface geophysical techniques to detect and map, if it exists, a confining unit between the shallow and deep aquifers and to determine the feasibility of using these techniques in other areas of the Coastal Plain.

GEOLOGIC SETTING

The Burton recharge area is located in the southern coastal plain of South Carolina and is underlain by clastic and carbonate sediments ranging in age from Cretaceous to Holocene. This study addresses only the late Tertiary and Pliocene to Holocene sediments. Siple (1960), Hayes (1979), and Spigner and Ransom (1979) have provided much information on the Tertiary and older sediments found in the study area.

Structure

On a regional scale, two structural features have affected the deposition of Tertiary and post-Pliocene sediments (Fig. 2). The first is the Cape Fear Arch, one of the most prominent structural features along the central part of the Atlantic Coastal Plain. It is a general warp of the basement with an axial plunge to the southeast (Hayes, 1979). Farther to the southeast, this gentle uniform dip of the basement is interrupted by the Southeast Georgia Embayment. The embayment, which extends from slightly north of Charleston to the Peninsular Arch of Florida, was regarded by Maher (1971) as primarily a tectonically passive margin, with some downwarping. The embayment is generally featureless, with two exceptions: the Burton High (Siple, 1960) — later renamed the Beaufort Arch (Colquhoun and others, 1969), and the Ridgeland Trough (Heron and Johnson, 1966).

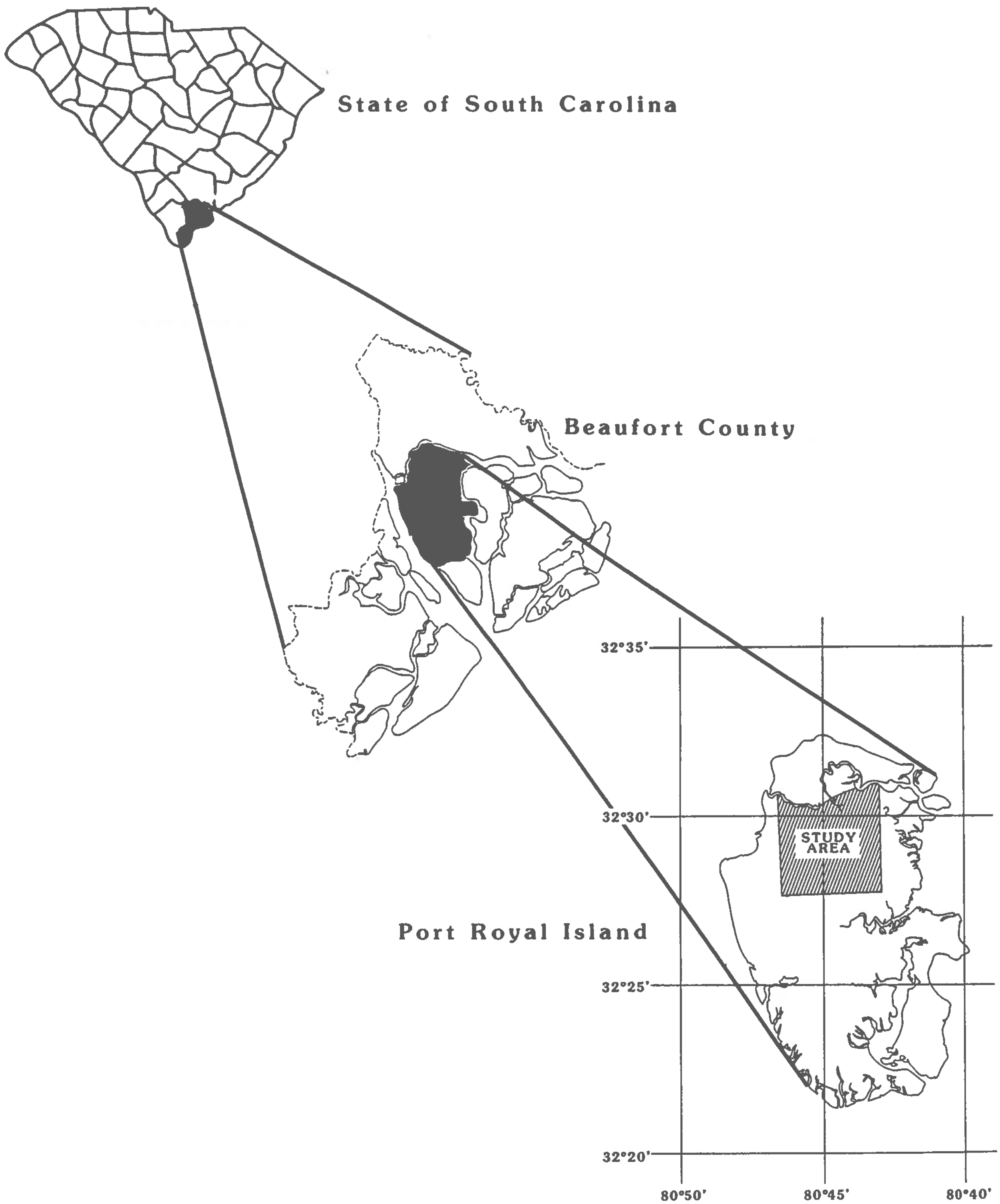

Figure 1. Location of Port Royal Island and the Burton recharge area.

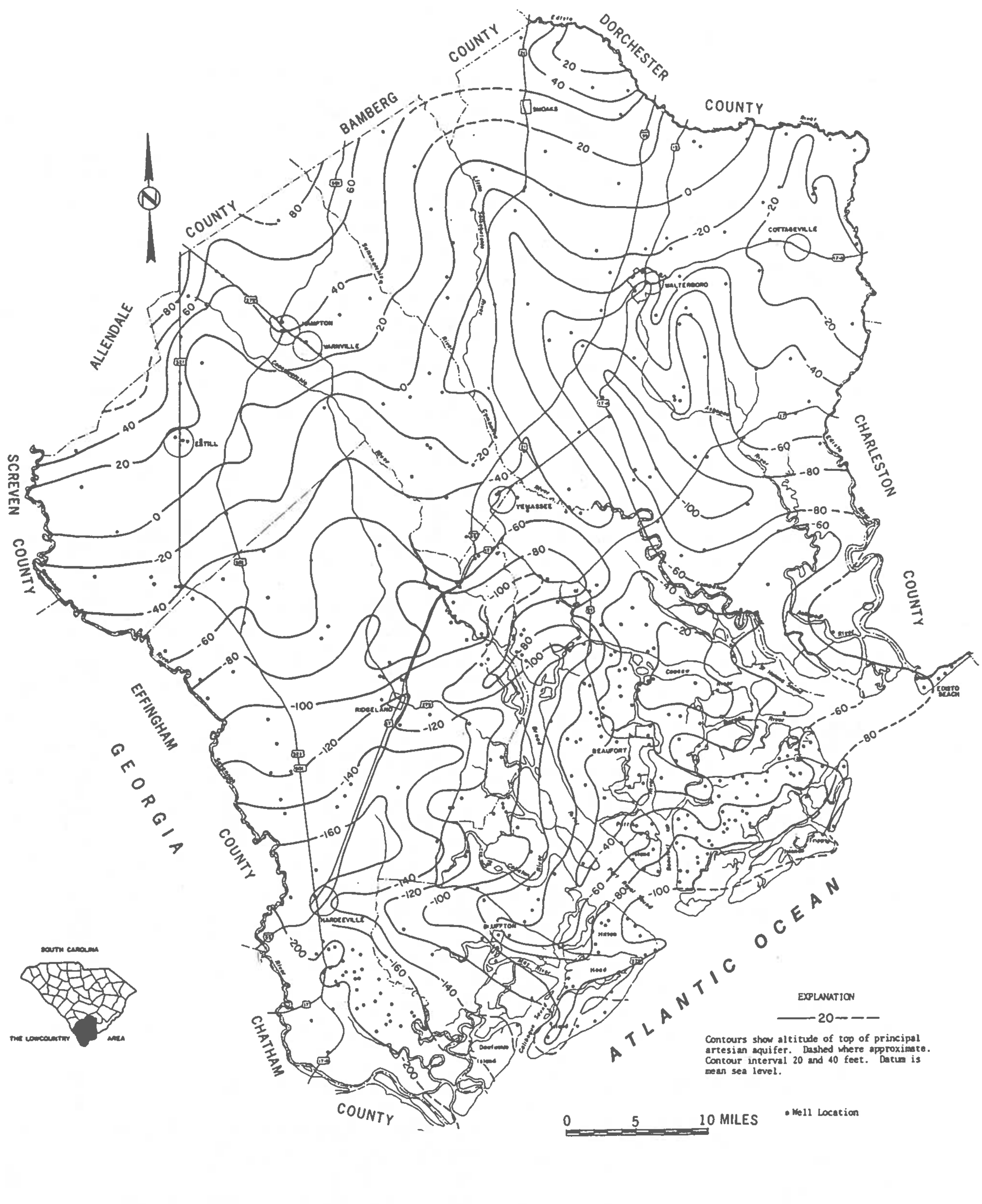

Figure 2. Structural map of the top of the Ocala Formation (from ~~Siple, 1960~~ Hayes, 1979).

The Beaufort Arch was first recognized by Siple (1960), who generated a structure-contour map of the top of the Ocala Limestone (Fig. 2) showing that the limestone is within 25-30 feet of the surface on Port Royal Island. Colquhoun and others (1969) postulated that the Beaufort Arch and associated Ridgeland Trough to the north are the result of tension forces that existed during Cenozoic time and possibly through the Tertiary.

The Ridgeland Trough was first recognized by Heron and Johnson (1966). The dip of the Coastal Plain sediments, which generally is seaward at about 6-15 feet per mile, is reversed in the Ridgeland Trough where the sediments dip landward. The Miocene Hawthorn Formation (Fig. 3) normally averages about 100 feet thick in the Ridgeland Trough, indicating that the trough was pre-Miocene and was most likely formed during the latter part of the Eocene.

Tertiary Stratigraphy

Eocene Series

In the study area, the Eocene consists of the Black Mingo Formation, the Santee Limestone, and the Ocala Limestone. The Ocala Limestone is the principal aquifer and, to some extent, controls the areal extent of the Hawthorn Formation. For a detailed description of the Eocene formations, see Siple (1960), Spigner and Ransom (1979), and Hayes (1979).

The Ocala Limestone is subdivided into an upper and a lower unit (Siple, 1960) (Fig. 3). At the time of Siple's study, the Ocala Limestone was considered to be of Claiborne age and was regarded as equivalent to the Santee Limestone. Davies and others (1989) interpreted the upper and lower units as of late Eocene (Jackson) age, making the two units equivalent to the Ocala.

The upper unit of the Ocala consists of highly permeable bioclastic limestones ranging in thickness from zero to 20 feet. In the Burton recharge area, the upper unit is the principal aquifer, but north-northwest of the Burton recharge area, the upper unit grades into a less permeable, clayey to silty, semi-restricted, low-energy limestone.

Throughout the study area, the lower unit of the Ocala is a sandy, silty, clayey, low-permeability limestone that ranges in thickness from 200 to 600 feet (Siple, 1960; Hayes, 1979; Spigner and Ransom, 1979).

Miocene Series

The Miocene Hawthorn Formation (Cooke, 1936; Siple, 1960) unconformably overlies the Eocene Ocala Limestone in the vicinity of the Beaufort Arch and the Burton recharge area (Fig. 3). It ranges in thickness from zero to 100 feet, with the greatest thickness occurring in the Ridgeland Trough to the north of the study area. In the Burton recharge area, the Hawthorn Formation is composed predominantly of olive-gray clay ranging in thickness from zero to approximately 25 feet. When present, the Hawthorn separates the shallow aquifer from the limestone aquifer. Well cuttings and electrical characteristics indicate that this composition of the Hawthorn may change over short distances and become more silty and sandy. North and south of the Beaufort Arch, the Hawthorn Formation is composed of an upper unit of clay with phosphatic grains, a middle unit of sandy dolomitic limestone, and a lower unit of silty clay. In areas where the Hawthorn is composed of multiple units, it contains not only a confining unit — as in the area of the Beaufort Arch — but also an aquifer (Hayes, 1979; Comer, 1968).

Pliocene to Holocene Series

The post-Miocene sediments in the Beaufort area comprise the Duplin Marl, of Pliocene age, and predominantly sandy, unconsolidated Pleistocene and Holocene sediments (Fig. 3). The Duplin Marl probably is absent over the Beaufort Arch (Burton recharge area), and Siple (1960) considered it to be absent over most of Beaufort County. Where present, it is a sandy, fossiliferous, and slightly phosphatic unit. In the vicinity of the Burton recharge area, the Pleistocene and Holocene sediments lie either directly on the Miocene Hawthorn Formation or on the Ocala Limestone.

The Pleistocene and Holocene consist mostly of very fine to fine quartzose sand interbedded with lenses of clay and silt. Occasionally, the sand may become silty or clayey, but this does not appear to be laterally or vertically continuous. The Pleistocene and Holocene sediments constitute the shallow aquifer system in the Burton recharge area. These sediments and their depositional history are discussed in detail in the section on results of the geophysical survey.

METHODOLOGY

The effect of depositional environment on a large, multi-county area is minimal; however, it does become a major factor when trying to determine the geometry and size of a local recharge area or the direction in which ground water will migrate over a small area. Depositional environments consist of subenvironments called depositional facies; for example, a back barrier island depositional

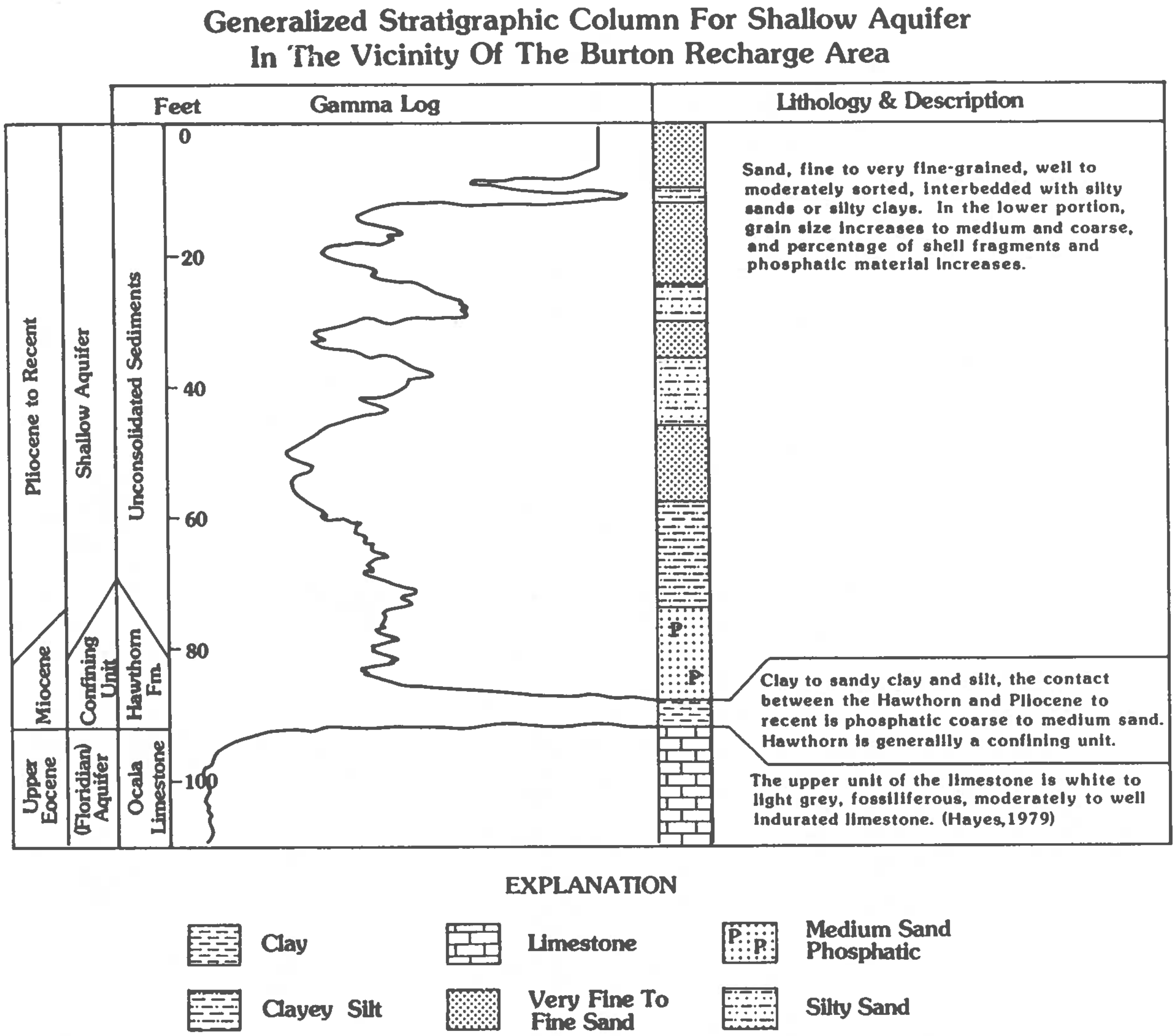

Figure 3. Generalized stratigraphic column and gamma-ray log response of the sediments of the shallow aquifer, the confining bed, and the upper unit of the Ocala Limestone.

model would consist of tidal channel facies, abandoned channel facies, and salt marsh facies. Depositional facies control the texture of the sediments; for example, the sediments deposited in a continuous high-energy environment, such as upper shoreface sediments, generally consist of fine-grained, well sorted sand with very little clay or silt. In this type of facies, porosity and hydraulic conductivity values are consistent in both vertical and horizontal directions. In an environment in which the energy level fluctuates — such as a back barrier environment, the tidal channel facies consist predominantly of fining-upward sand. Laterally, the sand generally grades into silt and clay of the marsh facies. Porosity and hydraulic conductivity are high in tidal channel deposits but low in the marsh deposits. Therefore ground water will flow through the area of less resistance — the channel deposits.

As each depositional facies also has a particular geometry, the consequence is that a model of a particular depositional environment consisting of a group of characteristic depositional facies will allow the investigator to predict the geometry and, to some extent, the direction of high and low hydraulic conductivity zones. This knowledge can be used to locate sites for pumping tests where the maximum amount of data can be obtained with the least number of test sites.

Most geologic studies involved in developing depositional models, for a particular formation or several formations, utilize either available well and borehole data or field information obtained from a series of borings or wells. The lithology and/or geophysical data from wells and borings are used to construct a series of geologic sections, which provide information on the lateral and vertical distribution of individual facies used to construct a depositional model. As the cost of drilling has increased substantially because of increased regulation, other methods of geological investigation must be explored and tested for effectiveness and feasibility. Therefore, surface geophysics has been selected as an alternative method of collecting subsurface geologic information. Although surface geophysics will not replace the drilling of test holes, the use of these techniques can reduce the number of wells or borings required for a comprehensive geologic study. In the present study, two surface geophysical techniques were employed — DC resistivity and multichannel seismic refraction.

Resistivity works on the theory that the sediments which constitute the subsurface geology have differing characteristics of resistance to the flow of electrical current, and that this can be measured. Factors affecting resistance include: the amount of space between particles (porosity), the degree of interconnection between the spaces (permeability), and the amount and conductivity of the fluid contained in the pore spaces. To determine DC resistivity in an ideal situation, four electrodes are placed in the ground, with the outer pair being the current electrodes and the inner pair being the potential electrodes (Fig. 4). If an electrical current is injected into a three-dimensional body such as the earth, the electrical current flow path from one current electrode to the other current electrode is not a straight line between the two current electrodes; rather, as the current flow spreads out in the subsurface, it radiates from one electrode and converges on the other, where it exits the system. The subsurface geology offers some resistance to the current flow, resulting in a drop in the potential field (voltage), which decrease is measured between the two inner, potential, electrodes. If the subsurface were homogeneous, the potential drop will be the same radial distance from either current electrode. The hemisphere formed at any given distance from a current electrode will be a surface on which all points have the same potential (Minning, 1973). This is the situation only for short electrode spacings. In Figure 4, each potential electrode lies on an equipotential hemisphere. The potential drop (voltage) is the measure of the volume of the earth that is between the two potential electrodes. Therefore, if the spacing between the electrodes is increased, the penetration of the electrical current is extended (Fig. 5). Knowing the amount of current being applied, the drop in the potential field, and the electrode spacing permits calculation of the apparent resistivity for a given depth. The apparent resistivity is an average for all the sediments encountered by the current flow. Although the apparent resistivity is an average, its value is influenced primarily by the sediments encountered near the equipotential line nearest the potential electrodes. As the distance increases, both vertically and laterally, away from the potential electrodes, the effect of the sediments not directly under the potential electrodes diminishes.

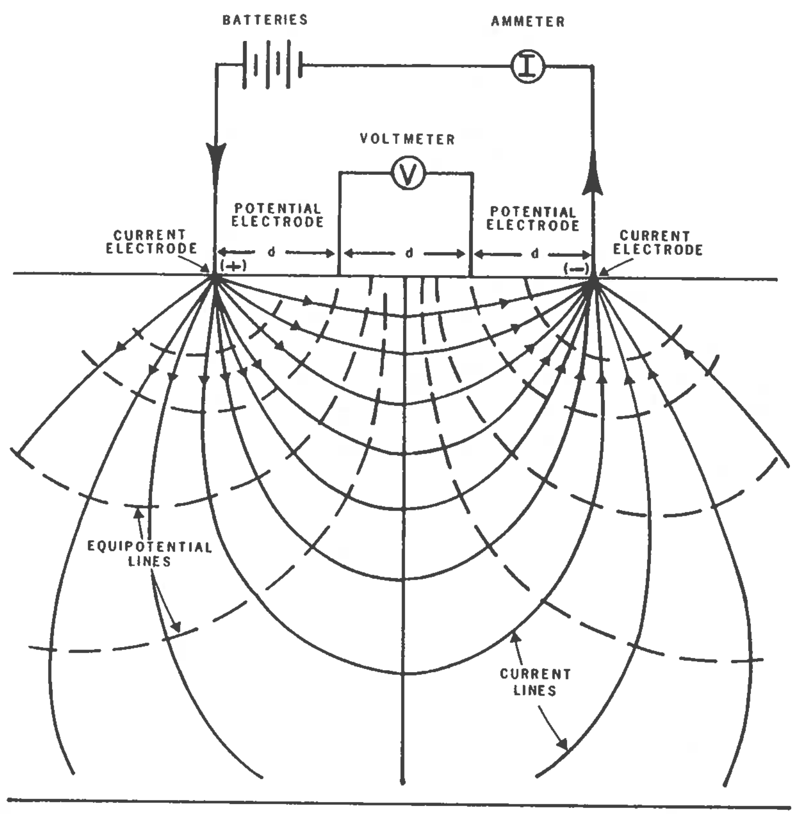

Figure 4. **Schematic diagram showing the basic concept of resistivity measurements, path of current flow, and equipotential lines (from Minning, 1973). Apparent resistivity values are calculated from the measured voltage and current and the spacing between electrodes, as shown in the equation a=2 A V/I, where a is apparent resistivity (ohm/m or ohm/ft), A is A-spacing (m or ft), V is potential (volts), and I is current (amperes).**

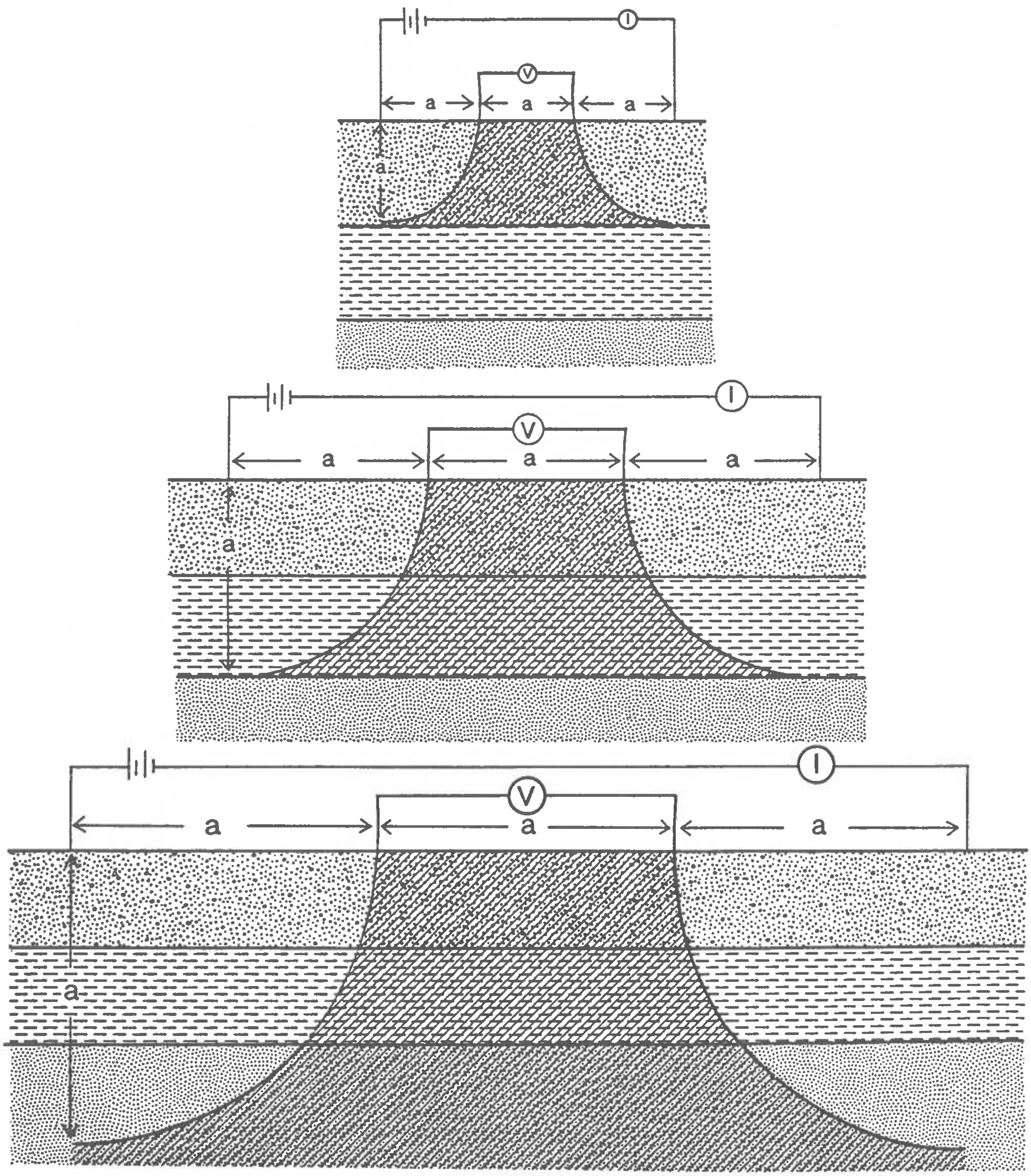

Figure 5. **Schematic diagram showing that the greater the electrode separation, the greater the depth of investigation (Minning, 1973).**

Surface electrical resistivity surveys generally utilize two field techniques: vertical electrical soundings (VES) and horizontal profiling. VES is used to determine vertical changes in resistivity in the geologic section at a given point. The technique involves taking a series of resistivity measurements at a given point and, with each successive measurement, increasing the AB/2 spacing (distance between individual electrodes) (Fig. 5). Two electrode configurations were tried at the beginning of this project to determine which technique could provide the most accurate subsurface data.

One configuration, the Wenner Array, consists of two current electrodes and two potential electrodes with equal A-spacings between all the electrodes (see Figure 4). The other configuration, the Schlumberger Array, also uses four electrodes (two current and two potential); however, the spacing between the current and potential electrodes in the Schlumberger Array is 3 to 5 times larger than the spacing between the two potential electrodes (Fig. 6). The Schlumberger Array has several advantages over the Wenner. The spacing between the potential electrodes is much smaller than the distance between the potential and current electrodes, thereby reducing to some extent the lateral variations in resistivity in the shallow subsurface; and the potential electrodes remain close together, allowing a slightly greater probing depth than does the Wenner sounding for an equal A-spacing (Zohdy and others, 1974). For those reasons, the Schlumberger Array was used for all the VES measurements in this study. In theory, the greater the A-spacing the greater the depth of investigation of the subsurface. But this theory is effective only in a homogeneous subsurface environment or with shallow investigations. With deeper investigations (greater AB/2 spacing), the assumption that the subsurface geology at depth is homogeneous is not tenable, and thus the assumption that the length of the AB/2 spacing is equal to the depth of investigation is not necessarily true. For example, electrical properties dictate that electricity will flow from a high-resistivity layer to a lower-resistivity layer. If there is a low-resistivity layer at depth, the current injected into the ground will flow toward the lower-resistivity layer — thereby increasing the apparent thickness of the higher-resistivity layer that is above the lower-resistivity zone. Because of heterogeneity in subsurface lithologies, the apparent resistivity measurements taken in the field must be converted into true resistivity, usually by curve matching, which involves determining the number of different resistant layers encountered in the subsurface and, based on the number of layers, matching the field curve to published theoretical curves. Where the theoretical curves match the measured curve, that point is the true resistivity value for that layer.

In this study, computer-generated theoretical curves were used to match the field curves. The large amount of data generated in this project made hand calculation of the true resistivity values impractical, so the Interplex resistivity modeling program (RESIX) was used. This program uses forward and inverse methods to obtain the true resistivity and thickness of individual subsurface layers. The forward model allows the operator to select the number of layers, the thickness of the layers, and the resistivity values for each layer from the field data. Table 1 presents resistivity field data from a VES; eight layers were selected, as was the thickness of each layer. In most cases, the resistivity value assigned to each layer is the highest value of that particular layer. For the resistivity of each layer assigned — for example, Layer 1 in Table

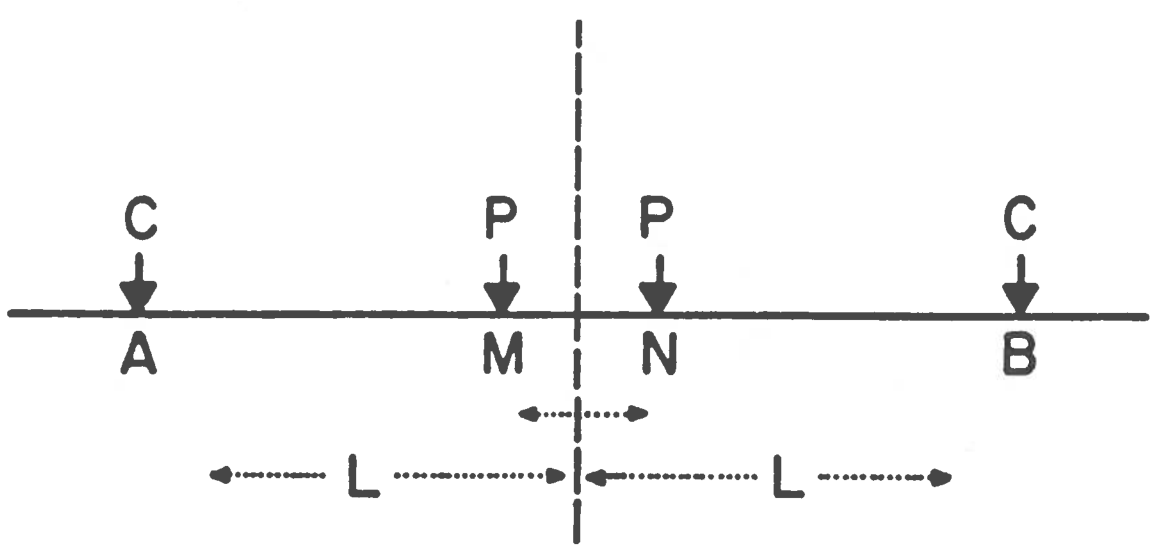

Figure 6. **Schematic diagram showing the electrode configuration for the Schlumberger Array. Take note that the potential electrodes (P) are relatively close to each other in relation to the distance between the potential and current (C) electrodes (from Benson, 1982).**

Table 1. Resistivity field data.

Field Data				
Spacing (ft)	Resistivity (ohm/ft)	Layer	Thickness (ft)	Resistivity (ohm/ft)
10.00 20.00	350.0 261.5	1	20	350.0
30.00 40.00	163.0 115.0	2	20	163.0
50.00 60.00 70.00 80.00	88.00 71.50 61.50 51.50	3	40	88.0
90.00 100.00 110.00 120.00 130.00	46.50 39.50 34.00 29.50 24.50	4	50	46.5
140.0 150.0	21.00 18.00	5	20	21.0
60.0 170.0 180.0 190.0	15.50 13.50 11.50 10.50	6	40	15.5
200.0	8.50	7	∞	8.5

1, the forward command is initiated and the program calculates the synthetic curve for the layered model selected by the operator for a given set of field data. Upon completion of the calculations, the model is plotted and the synthetic curve is plotted with the field data. Figure 7A shows the model and synthetic curve for the field data given in Table 1. In this case, the synthetic curve has been plotted above the field data because each layer was assigned the highest possible value for that particular layer. Although the synthetic curve values are higher, the basic shape of the synthetic curve is similar to that of the field curve (Fig. 7A). Once the general shape of the synthetic curve is similar to that of the field curve, the next phase of modeling can proceed. Inverting the forward model through several iterations minimizes the least-squares error between the field data and the synthetic curve. As can be seen in Figure 7B, the synthetic curve matches the field data. The resulting resistivity values and the thickness of individual layers are shown in Table 2, and this model is the best fit for the field data. If a model has over four layers, which is about the maximum number of layers that can be calculated by hand curve matching, and even though the field data and synthetic data match as well as in the example, there will be some question about whether this model is correct for the geology. Therefore, all geologic information for the area must be used in conjunction with the resistivity data in order to develop a workable model.

The second resistivity technique is surface resistivity profiling, which involves taking measurements with fixed electrode spacing. Generally, the electrode A-spacing is three to four times the depth of investigation (Zohdy and others, 1974; Benson and others, 1982; Van Nostrand and Cook, 1966). In this study, resistivity profiling was used at only two locations because of local culture interference such as water mains and buried cables.

The second geophysical technique used in this study was shallow multichannel seismic refraction. Seismic refraction surveys were used primarily as a tool to determine depth to the top of the Ocala Limestone or the top of the Hawthorn clays. Seismic refraction techniques measure the time it takes a compressional sound wave generated by a sound source other than nature to travel through the different sediment layers in the subsurface and back up to detectors on the land surface (Haeni, 1984) (Fig. 8). The technique is based on Snell's Law, which governs the refraction of sound or light waves across

Table 2. Resistivity values and layers after forward modeling.

Layer	Resistivity (ohm/ft)	Thickness (ft)
1	400.0	14.55
2	76.79	38.78
3	64.79	20.80
4	20.68	22.59
5	13.17	9.48
6	9.35	9.34
7	2.03	

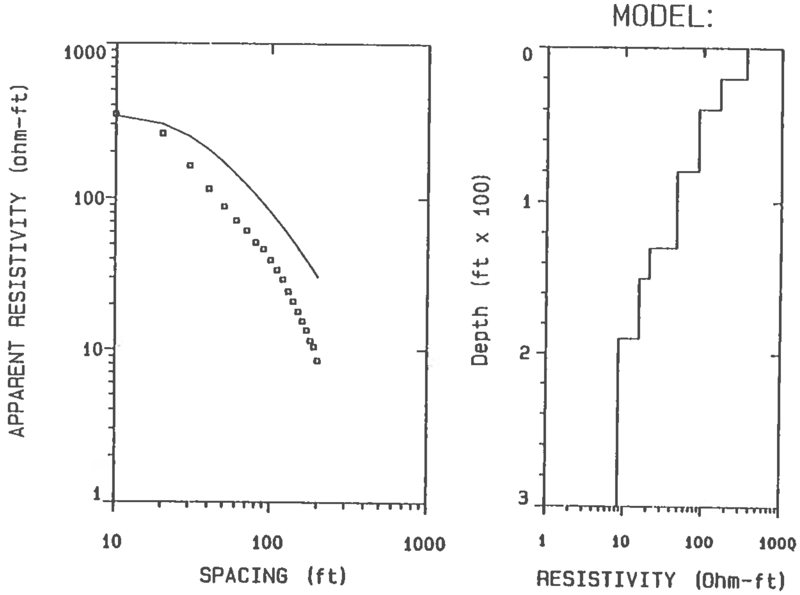

Figure 7A. **Diagram showing the field resistivity values (squares) with a synthetic curve developed from the forward model (solid line), and the true resistivity values also derived from the forward model.**

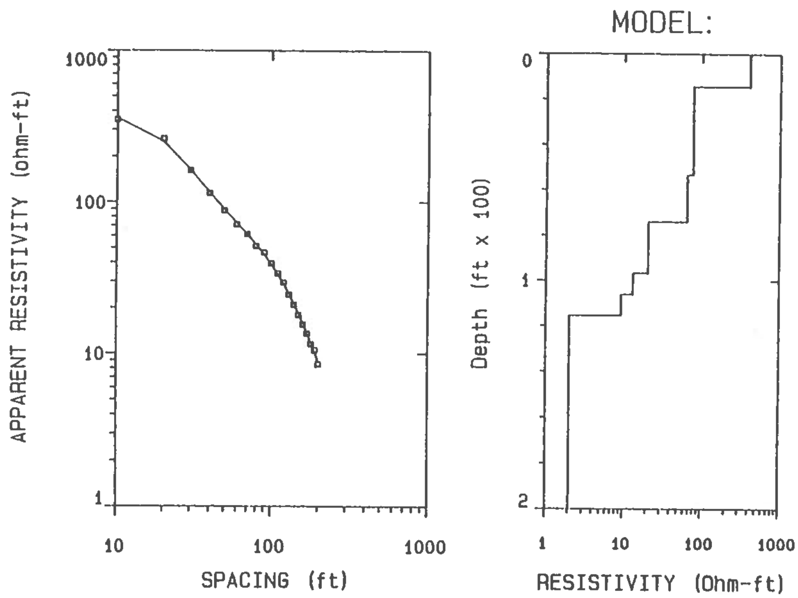

Figure 7B. **Diagram showing the forward resistivity model after a series of inversions. Notice that the synthetic curve (solid line) matches the field data (squares); furthermore, note that the true resistivity values and thicknesses of the various layers have also changed.**

the boundary between layers of different velocities. It determines that, when a sound wave propagates through one layer and the next layer encountered has a faster velocity than the previous layer, some of the energy is refracted, or bent, and part is reflected back into the first layer. The refracted wave will move along the boundary between the two layers, generating new sound waves that are of the same velocity as in the first layer. As the wave approaches the critical angle, it is refracted back to the surface and detected by a series of geophones laid on the land surface in a geometric array (Fig. 8). The thickness of Layer 1 and the velocity of Layer 2 can be calculated if the distance from the sound source to the geophones and if the time for the sound wave to penetrate to Layer 2 and return to the surface are known. These calculations can be done by using intercept times and crossover distance-depth formulas. For details on the formulas and method, see Dobrin (1976) and Haeni (1986).

The database for this project consisted of approximately 80 vertical electrical soundings, two electrical profile lines, 13 wells and borings, and 16 seismic refraction surveys (see Fig. 9). The well and borehole data and the model vertical resistivity data were used to construct nine sections across the study area (see Plates 1-3). The seismic data were used to determine the depth to limestone or depth to clay

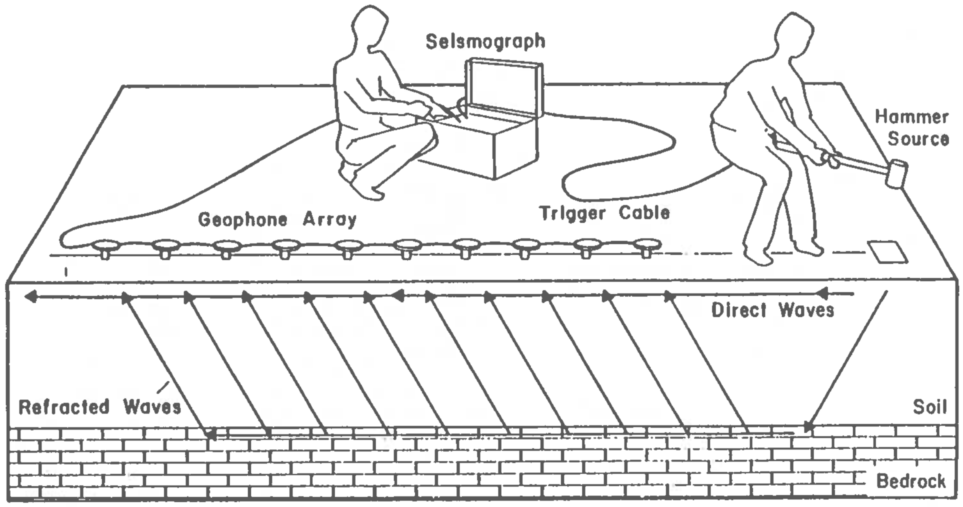

Figure 8. **Schematic diagram showing the principle of seismic refraction, the path of the direct waves, and refracted seismic waves in a two-layered model (after Benson, 1982).**

within the Hawthorn Formation; these data are listed in Table 3. One can see from these data (Table 3) that there are velocity variations in the sand that constitutes the shallow aquifer, most likely owing to variations in the admixture of clay or silt — with higher velocities occurring in silty or clayey sand. The limestone also shows considerable variation over the study area (Table 3) — a reflection of the degree of consolidation of the limestone, or its porosity. The seismic interpretations are based on the velocity and correlation with either resistivity or well data or both. Sections were generated and correlated and isoresistivity contour maps were constructed — one from raw field data (apparent resistivity; see Fig. 10) and one depicting the true-resistivity values (see Fig. 11) at approximately 80 feet below the land surface -- the Hawthorn Formation. A structure-contour map for the top of the Ocala Limestone was generated from a combination of resistivity data, well and borehole data, and seismic data (see Fig. 12).

DESCRIPTION OF GEOLOGIC SECTIONS

Nine geologic/geoelectric sections were constructed across the Burton recharge area to determine vertical and lateral variations in the the shallow aquifer (Pleistocene and Holocene), the lateral extent of the Hawthorn Formation, and the depth to the top of the Ocala Limestone. The primary database for construction of the sections was vertical electrical soundings (Fig. 9). In interpreting geoelectric sections, one must understand what causes resistivity values to increase or decrease. In general, these values decrease as porosity, permeablibity, and water conductivity increase. A decrease in grain size also causes a decrease in resistivity values; an increase in grain size, as well as the absence of fluid in sediments lying above the water table, causes an increase in resistivity. Increases in silt or clay will generally cause decreases in resistivity values because of reduced permeability and because of electron exchange from particle to particle that occurs in a highly conductive material (Minning, 1973). Not only grain size and amount of clay affect resistivity values, water quality does as well. If the water is conductive, the resistivity values will decrease. Conductivity changes primarily because of an increase in the amount of dissolved solids in the water; those that most affect resistivity are chlorides (salt) and iron, which are highly conductive minerals. Chlorides do not appear to be a problem, at least in the shallow aquifer; test boring data on the Burton indicate that iron is present and occurs in distinct zones in the subsurface.

Section A-A'

A-A' is a north-south trending section (Fig. 9, Plate 1). The lowermost unit is the Ocala Limestone, the resistivity values of which range from 0.1 to 13 ohm/ft, which are generally considered low for limestone. These low values are probably caused by either iron in the water or iron that has precipitated out of solution and is lining the pore throats. Even if there were not any iron present, the resistivity values would be lower than expected for limestone. The resistivity value at a given AB/2 spacing is an average value of not only the layer that is being measured at a given AB/2 spacing, but also the

Table 3. Seismic refraction velocities and interpretations.

Burton sta. no.	Layer 1 Velocity (ft/sec)	Layer 1 Interpretation	Layer 2 Velocity (ft/sec)	Layer 2 Interpretation	Thickness layer 1 (ft)
1	3750	saturated sand	9375	limestone	98
2	2916	saturated sand	5288	saturated sand	56
3	3526	saturated sand	10,416	limestone	96
4	3676	saturated sand	7638	silty/sandy clay	73
5	3333	saturated sand	9166	limestone	85
6	3378	saturated sand	6547	limestone	70
7	3333	saturated sand	5500	saturated sand	61
8	3353	saturated sand	5681	sand	69
9	3378	saturated sand	5288	saturated sand	57
10	3676	saturated sand	16,500	limestone top	99
11	3676	saturated sand	4824	saturated sand	45
12	4166	saturated sand	4824	saturated sand	33
13	4069	saturated sand	6769	limestone	87
14	3378	saturated sand	5392	saturated sand	59
15	3205	saturated sand	5729	sand	66
16	3378	saturated sand	5500	saturated sand	61

overlying layers. Therefore, although the resistivity value of the limestone would be higher than that of the overlying sands, it would be suppressed because of the low resistivity of the sands. As discussed in the methodology section, the resistivity value for a given AB/2 spacing is an average of the total volume of the earth through which the current is flowing.

Directly above the limestone is another low-resistivity unit (<1.0 ohm/ft), which is present near the north end of the section (VES-62, -73) and in the southern half (VES-12, -13, -14, -15; wells BFT-1906, BFT-1728). This interval is interpreted as clay or silty clay; it appears to be a remnant of the Hawthorn Formation. Directly above the clay in the vicinity of VES-61 and VES-56 and in direct contact with the limestone are several units interpreted as sand; the resistivity values range from 1.0 to 2,750 ohm/ft. The middle units, with resistivity values ranging from 12 ohm/ft (VES-62) to 1.0 ohm/ft (VES-12 and -13), appear to be of very fine sand. This correlates with the data from wells BFT-1906 and BFT-1728. The low-resistivity values are attributed to several factors: *(i)* the sand is very fine grained; *(ii)* silt or clay is present within the matrix of the sand; and *(iii)* the ground water within the sand has become conductive due to an increase in iron or iron-rich minerals. As discussed in the section on geologic setting, the Pleistocene and Holocene deposits in the vicinity of the Burton recharge area were deposited in shallow marine or coastal-plain environments. Colquhoun (1971) demonstrated that the sea transgressed and regressed numerous times during the Pleistocene, thereby causing a stacking of tidal inlets and channels — upper shoreface deposits on lower shoreface deposits and the reverse. It appears that erosion of the Hawthorn clay most likely occurred during a low stand of sea level. As the sea began to rise and transgress over the Beaufort Arch, the Hawthorn was eroded away and replaced with very fine- to fine-grained nearshore to upper shoreface sand.

In the vicinity of VES-61, seismic refraction data (Table 3, sta. B-13) suggest that the limestone is approximately 87 feet below the land surface. The velocity of the limestone is very similar to the velocity of saturated sand. The upper 20-30 feet of the limestone is extremely porous, therefore the velocity should be similar to saturated sand. In contrast, the sandy or silty clay appears to have a higher velocity than the sand or limestone. Borehole data indicate that the clay in the Hawthorn is semi-compacted and has a higher velocity than either the sand or

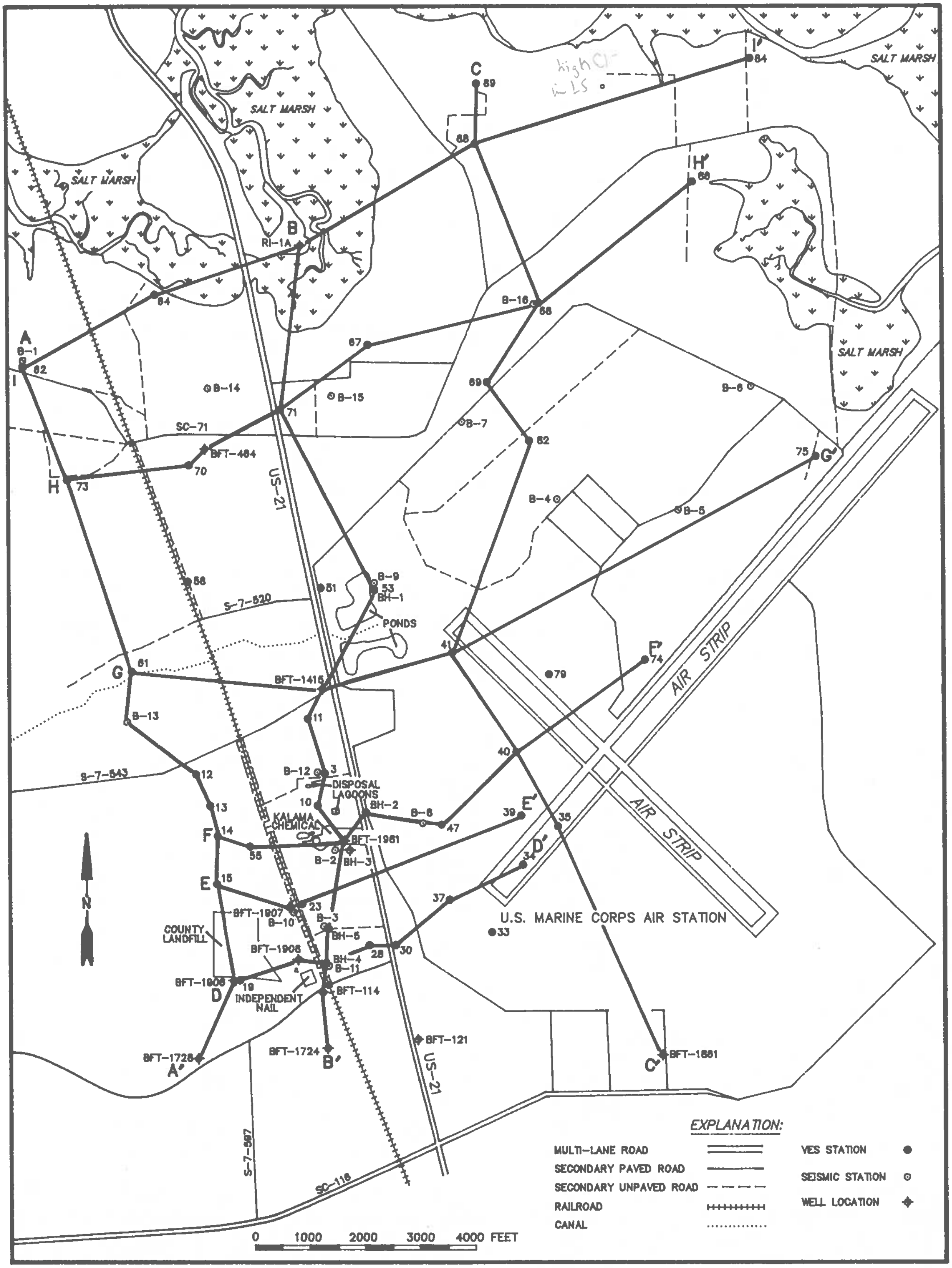

Figure 9. Locations of the vertical electrical soundings (VES), seismic-refraction stations, wells, and geologic sections.

limestone. From seismic, electrical, and borehole data, therefore, it was determined that the Hawthorn has been eroded away and the sand was deposited directly on the limestone.

The Hawthorn clay appears to be present to the north (VES-72 and -73) and to the south (VES-61). Low- to moderate-resistivity layers lie directly above the clay or limestone; they have been interpreted as sand. The low-resistivity sand has values ranging from 12 ohm/ft to 1 ohm/ft. Borehole data suggest that the sand contains limonite or an unidentifiable secondary iron-rich mineral, and the individual sand grains are coated with an iron precipitate. The presence of iron either coating or within the pore waters would make that zone highly conductive, substantially reducing the resistivity values. A thin layer of moderately high-resistivity sand lies above the low-resistivity sand, ranging from 36 ohm/ft (VES-73) to 19 ohm/ft (VES-61). The increase in resistivity values appears to be the result of a decrease in the conductivity of the pore waters and a slight increase in grain size. The increased resistivity within the unit, excluding values higher than 100 ohm/ft, is most likely due to a slight increase in grain size and a reduction in water saturation. The uppermost layer is a high-resistivity sand that thins to the south. The upper part is composed of dry, fine-grained, quartzose sand with little or no clay and silt, which would account for the high resistivity values.

Section B-B'

B-B' is located east of section A-A' and is also a north-south trending section; it begins in the north at well BFT-1909 and terminates in the south at well BFT-1724 (Fig. 9, Plate 1). The base of the section is the Ocala Limestone. As in section A-A', the resistivity values are generally low for limestone and also show lateral variations in values. Again, the low values are possibly due to the high porosity and permeability of the limestone and the presence of increased conductivity of the pore waters. Directly above the limestone is a series of mostly low-resistivity zones with resistivity values of 1.0 ohm/ft or higher when correlated with data from the adjacent wells (BFT-1450, -1981, -114, -1724); these low-resistivity zones are interpreted as sand. It appears that the low resistivity values are caused by a combination of increasing iron in the pore waters and iron coating individual grains. The Hawthorn appears to be absent in the north (well BFT-1909, VES-71 and -53; borehole BH-1) and is also absent at well BFT-1981. The unit appears to be present in the middle of the section in the vicinity of well BFT-1450 and VES-11, -3,and -10, and also to the south in boreholes BH-3, -5, and -4.

The increase in thickness of the Hawthorn in VES-11, -3, and -10 is mostly likely not an actual increase, but rather a combination of Hawthorn clay at the base, in direct contact with the limestone, and partially iron-cemented sand in the upper portion. A test borehole drilled by the South Carolina Department of Health and Environmental Control in the vicinity of VES-3 found some of the sand in the shallow aquifer to be partially cemented with an iron-rich mineral (R. Knox, pers. comm., 1988). A seismic survey was conducted adjacent to VES-3 and the first layer was calculated to be 33 feet thick (Table 3); the difference in velocity between layers 1 and layer 2 is approximately 650 ft/sec. Although the velocity difference is small, it suggests that the sand in layer 2 is slightly denser. There is a drop in resistivity values at about 33 feet from the land surface in VES-3. This increase in velocity and drop in resistivity values suggests that iron is possibly coating the sand grains and possibly in solution in the pore waters. Directly above the limestone and the Hawthorn clay is a low- to moderate-resistivity sand. Lithologic data from BH-1, -3, -4, and -5 indicate that clay content and grain size do not vary substantially in the low- to moderate-resistivity sand. Where the low-resistivity zones begin, according to data from BH-3, -4, and -5, the sand appears to contain limonite and the individual grains appear to be coated with an iron precipitate. The lithologic data strongly suggest that the low- to moderate-resistivity values in the sand are caused by variation in water quality, rather than by textural changes. The geometry of the low- to moderate-resistivity sand may be controlled by depositional facies. The most likely source of the iron is the decay of organics within the sand. The areas of highest iron concentration (low resistivity values) today were probably the most porous in the past. For iron to precipitate, the concentration must exceed saturation, which would involve a large volume of water flowing through, suggesting great porosity. The high resistivity values of the upper layer observed at all of the VES stations on section B-B' are caused primarily by a combination of a reduction in water saturation and a slight increase in grain size.

Section C-C'

C-C' is the easternmost north-south trending section in the study area (Fig. 9, Plate 1); it begins at VES-88 in the north and terminates at well BFT-1861 in the south. In the Ocala Limestone, the lowest unit, resistivity values are higher than on sections A-A' or B-B'. These increases, although slight with the exception of VES-68, suggest that porosity and permeability are increasing slightly, or the higher values may indicate a change in water quality. The abnormally high values at VES-68 appear to be a modeling, not a geological, problem. Above the limestone, the low-resistivity zone of Hawthorn clay occurs as an isolated patch at VES-68, and the zone reappears slightly north of VES-40 and continues southward at least to well BFT-1861. Elsewhere, the low-resistivity clay (less than 1.0 ohm/ft) has been eroded and replaced by a low-resistivity sand during a low stand in sea level during the Pleistocene.

Directly above the Hawthorn clay and in the vicinity of VES-88, -69, -82, and -41, a low-resistivity sand is either directly above the limestone or the clay. As discussed previously, the low resistivity values in the sand are caused primarily by changes in water quality rather than by textural changes. The lithology described from well BFT-1861 suggests that the sand texture (grain size) changed only slightly. The lithology log and samples from boreholes in the area suggest that the low resistivity values for the sand are due to an increase in the conductivity of the pore water — that is, an increase in iron. The geometry of the iron-rich zones, as noted previously, is most likely controlled by depositional facies. The zones that now have the greatest concentration of iron were probably the most porous at one time. To the north in the vicinity of VES-68, -69, and -82 and to the south at VES-35, layers of moderately high resistivity values vary both laterally and vertically. These zones are interpreted as sand and, again, the high values appear to be related to water quality rather than to textural changes in the sand.

Above the moderately high-resistivity sand is a high-resistivity zone. To the south and north of VES-68 are thin zones of moderately high resistivity which, in turn, are overlain by high-resistivity zones. These variations are due primarily to differences in water saturation of the sand rather than to textural changes. The high-resistivity zone here, as in previous sections, is the zone of unsaturated sand with little or no water in the pores.

Section D-D'

D-D' is a west-east trending section (Fig. 9, Plate 2) that, like the Sections E-E', F-F', G-G', H-H', and I-I', appears to be either along depositional strike or slightly off the strike direction. The lowermost mappable unit is the Ocala Limestone. As in previous sections, the resistivity values are low for limestone, and they are highly variable — which seems typical for the study area. At VES-20, -28, and -30, the values for the limestone are higher than expected for the area, probably caused by a combination of slight textural changes in the limestone and changes in water quality. Above the limestone, the low-resistivity clay of the Hawthorn Formation is present on the western and eastern portions of the section. In the middle portion of the section, the Hawthorn clay has been eroded and replaced by moderately high-resistivity sand to the west (VES-20 and-28) and low-resistivity sand to the east (VES-30). It appears that the absence of clay is the result of erosion by rising sea level during the Pleistocene, and that clay was subsequently replaced by low-resistivity sand. The low-resistivity sand occurs from approximately the middle of the section at VES-30 eastward to VES-34. To the west at borehole BH-4, limonite was encountered in the samples, and seismic data (Table 3, sta. 11) from the same location show a velocity increase at approximately the same depth as the sand containing limonite was encountered. As resistivity data from the same location were not usable because of cultural interference, and the low-resistivity sand appears to pinch out at VES-28, the sand was patterned with the moderately high-resistivity sand on the basis of borehole samples. An extremely low-resistivity sand was encountered at VES-30, with a resistivity value of less than 1 ohm. This has been interpreted as sand, not clay, because of reports of zones in the sand that are almost completely cemented with iron precipitate (R. Knox, pers. comm., 1988). The lateral variation in resistivity values is, again, most likely caused by changes in water quality in the sand. As mentioned previously, this section contains a thin veneer of high-resistivity sand which, in this interval, is not attributed to textural changes but rather to changes in water saturation. This high-resistivity zone is above the water table.

Section E-E'

E-E' also trends west-east and is located north of Section D-D' (Fig. 9, Plate 2). In the Ocala Limestone (lowermost unit), resistivity values are low, which appears to be normal for the study area. The Hawthorn Formation clay is present from approximately the center of the section (VES-32) westward to the end of the section. The clay appears to have been eroded and replaced by low-resistivity sand beginning slightly east of VES-32. The low-resistivity sand has values ranging from 2 ohm/ft to as high as 9 ohm/ft. This variation in resistivity values is most likely the result of iron in the pore waters or iron-rich minerals that have precipitated out of the pore waters, rather than textural changes in the sand. Directly above the low-resistivity sand is a layer of moderate- resistivity sand that is absent at VES-32 but increases in thickness both to the west and east. The upper high-resistivity zone is unsaturated sand above the water table.

Section F-F'

F-F' trends west-east and is north of section E-E' (Fig. 9, Plate 2). The lowermost unit, the Ocala Limestone, is highly variable; values range from 0.1 ohm/ft to as high as 418.0 ohm/ft. The latter value is expected for a well-consolidated limestone. Directly above the limestone and at the westernmost end of the section at VES-14 is Hawthorn Formation clay. Slightly east of VES-14, the Hawthorn has been eroded and replaced by either low- or high-resistivity sand. Farther east, the Hawthorn is present beginning slightly west of VES-40 and extending east to the end of the section. The high-resistivity sand directly above the limestone in VES-47 and in well BFT-1981 appears to be a change in texture rather than water quality. Geologic samples from that interval in well BFT-1981 are fine- to medium-grained sand with abundant shell fragments and phosphatic grains. The grain size is coarser than in the sand above the interval, and the presence of the phosphatic grains and shell fragments suggests channel-lag deposits. The source of the phosphatic grains is erosion of the Hawthorn Formation. Directly above the high-resistivity sand is a low-resistivity sand. Lithologic sample descriptions from well BFT-1981 suggest that, within the low- and moderate-resistivity sand and the lower portion of the high-resistivity sand, the texture and amount of silt and clay do not vary enough to cause such a substantial drop in resistivity values. Therefore, the reduction appears to be the result of changes in water quality rather than in textural composition of the sand. The occurrence of high-resistivity values in the uppermost sand is a result of the sand being unsaturated.

Section G-G'

G-G' is north of section F-F' and is also a west-east trending section (Fig. 9, Plate 3). The resistivity values in the Ocala Limestone (lowermost unit) increase to the west but are still considered low for limestone. Most of the Hawthorn clay appears to have been eroded, with only a narrow section appearing in VES-75 and extending slightly westward. On the western side of the section, the limestone is overlain by a low-resistivity sand that has replaced the Hawthorn clay. As on previous sections, the resistivity values appear to be controlled primarily by the conductivity of the pore waters rather than by the amount of clay and silt and the grain size. The gamma-ray log on well BFT-1415 suggests that there is little vertical change in clay and silt content and no significant change in grain size. Therefore, the low- and moderate-resistivity sand is a function of the conductivity of pore waters rather than of textural changes. The unsaturated zone, again, has high resistivity values.

Section H-H'

H-H' begins in the west at VES-73 and extends east to VES-86 (Fig. 9, Plate 3). In the Ocala Limestone, the lowermost unit, resistivity values range from a low of 0.9 ohm/ft at VES-86 and VES-73 to a high of 807 ohm/ft at VES-68. The high resistivity value at VES-68 is about two times greater than expected for a limestone. The only plausible explanation is that a small, isolated, highly resistive layer is causing this high value. The low-resistivity Hawthorn clay is present at the west and east ends of the section. Most of the Hawthorn clay appears to have been eroded. At the west end of the section, the clay is present in VES-73; however, it has been eroded and replaced by a moderate-resistivity sand that is present in VES-70, and the log signature in well BFT-464 suggests a clean, fine- to very fine-grained sand. Directly above the moderate-resistivity sand is a low-resistivity sand that thins to the east between VES-67 and VES-68. At VES-68, the low-resistivity sand has been replaced by a moderate-resistivity sand. The low-resistivity sand reappears between VES-68 and VES-86 and increases in thickness to the west. As the low-resistivity sand thickens, the moderate-resistivity sand thins and pinches out at VES-86. The lenticular shape of the moderate-resistivity sand suggests the possibility that it was a channel sand. If it is assumed that the low resistivity values in the sand are more due to changes in the amount of iron present than to textural changes in the sand, then the low-resistivity zones were the preferred pathway of ground water movement. As discussed in previous sections, the area where there is the greatest accumulation of iron either coating the framework grains or still in solution is also the area where porosity and permeability were laterally and vertically consistent. This consistency would allow the large volume of water required for iron precipitation to pass through. The moderate-resistivity sand, on the other hand, may be due to either a slight change in grain size or a change in primary sedimentary structures (crossbedding) that slightly hinders the flow of water and lessens iron precipitation. The size and configuration of the moderate-resistivity sand suggest that it is a channel deposit. Above the moderate-resistivity sand is a thin layer of high-resistivity sand, which is above the water table — explaining the high value.

Section I-I'

I-I' is a west-east trending section (Fig. 9, Plate 3). As in the previous section descriptions, the lowest unit is the Ocala Limestone. The only low-resistivity clay of the Hawthorn Formation is at the far western side of the section, at VES-62. In the remaining portion of the section, the Ocala is overlain by low-resistivity sand. The low-resistivity sand has been further divided into two zones. The lower zone, in direct contact with the limestone, has resistivity values of 1-2 ohm/ft. The upper zone has slightly higher resistivity values — ranging from 12 to 4 ohm/ft. As in most areas where the low- to moderate-resistivity zones are in direct contact with the limestone, the resistivity values tend to be lower and to increase upward. If one accepts the idea that low-resistivity values are the result of increasing conductivity brought on by an increase in iron, then the low values in the limestone are also the result of an increase in conductivity brought on by a increase in iron. At VES-62, two layers of high-resistivity sand are separated by a zone of moderately high-resistivity sand. The high resistivity values in the lower layer of high-resistivity sand appear to be the result of increasing grain size rather than decreasing water saturation. The upper layer of high-resistivity sand is most likely due to a decrease in water saturation.

ISORESISTIVITY CONTOUR MAPS

One isoresistivity map was constructed from apparent-resistivity values (Fig. 10), and one from true-resistivity values derived from model data (Fig. 11). The apparent-resistivity map used values derived from an AB/2 spacing of 240 feet. The true-resistivity map used resistivity values from approximately 80 feet below the land surface, which appears to be the top of the Hawthorn Formation. When using raw data (apparent-resistivity data), the general rule is an AB/2 spacing of three to four times the actual depth of interest (Zohdy and others,1974); therefore, Figure 10 is a contour map of apparent resistivity using data from an AB/2 spacing of 240 feet — a depth of approximately 80 feet below the land surface.

Figure 10 is a contour map of apparent-resistivity values and Figure 11 is a contour map of corrected true-resistivity values. Apparent-resistivity values generally are lower than the true-resistivity values, although both maps represent the same stratigraphic interval. As previously discussed, the apparent-resistivity value is an average for the entire depth of investigation. Therefore, the low-resistivity values of the sand above the depth of interest influence the readings at that depth. The true-resistivity map consists of values that have been corrected for such influences as low-resistivity zones.

On Figure 10, the area within the 10- and 5-ohm/ft contours is interpreted as sand that has replaced the clay of the Hawthorn. The shape of this 10-5 ohm/ft contour area is elongated and sinuous, with its long axis trending north-south (Fig. 10). The basic shape of the 10-ohm/ft contour and samples from boreholes and wells suggest that deposition of the sand and subsequent removal of the Hawthorn clay was caused by channeling. The data derived from samples strongly suggest the channels are tidal. The presence of glauconite and abundant shell and skeletal fragments near the base of the channels also suggests a marine or marginal marine environment. Figure 11 is a contour map of true-resistivity values for an interval of 0 to 20 feet that is approximately 80 feet below land surface, or Hawthorn equivalent. The area between the 10-ohm/ft and 15-ohm/ft contours is interpreted as sand that has replaced the Hawthorn clay. The shape of the 10-15 ohm/ft contour area is similar to that of the 10-5 ohm/ft contour area (Fig. 10); however, the 10-15 ohm/ft area is more elongated and narrower. The difference in geometry between the 10-5 ohm/ft area on Figure 10 and the 10-15 ohm/ft area on Figure 11 is due to differences in both apparent- and true-resistivity values.

DEPOSITION IN THE BURTON RECHARGE AREA

Depositional History

The size and geometry of a recharge area may be controlled by the geology of an overlying shallow aquifer. In the Burton recharge area, the presence or absence of the confining bed is controlled by the depositional history of the overlying sediments of the shallow aquifer.

Two major factors affected erosion of the Hawthorn Formation (confining bed) and the deposition of sediments in the overlying shallow aquifer — formation of the Beaufort Arch and the numerous fluctuations in sea level that occurred during the Pleistocene. The Beaufort Arch probably formed either before or during the Eocene (Colquhoun, 1969), and it was a prominent high during Pleistocene deposition. It has been documented that sea level fluctuated greatly during Pleistocene time and the sea transgressed and regressed over the southern coastal plain of South Carolina. In the vicinity of the Burton recharge area, the overlying Pleistocene sediments appear to have been deposited in a shallow-sea environment, with lower and upper shoreface deposits predominating.

During a rise in sea level in early Pleistocene time, the southern coastal plain was inundated by

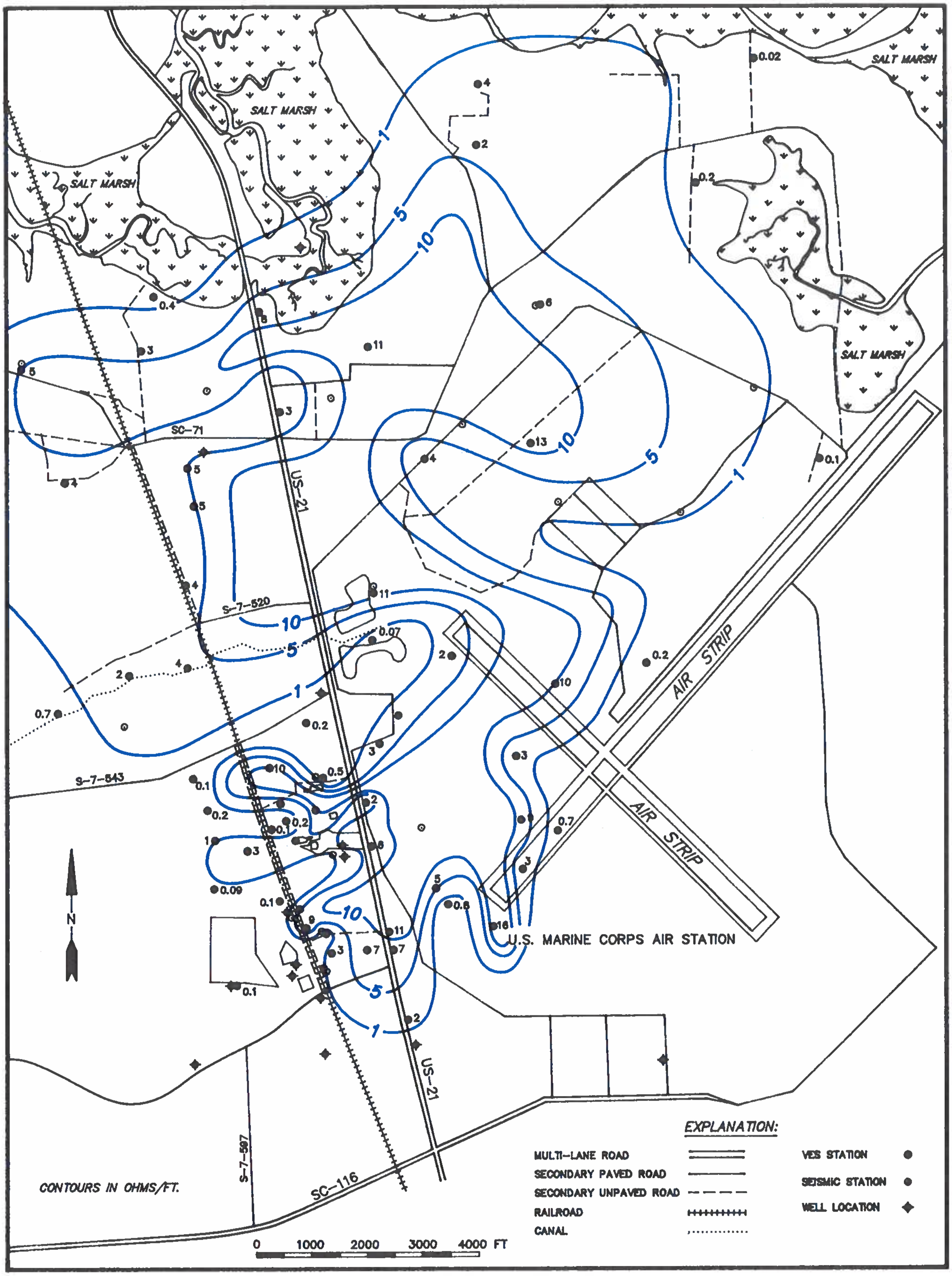

Figure 10. Contour map of apparent-resistivity values in the vinicity of the Burton recharge area.

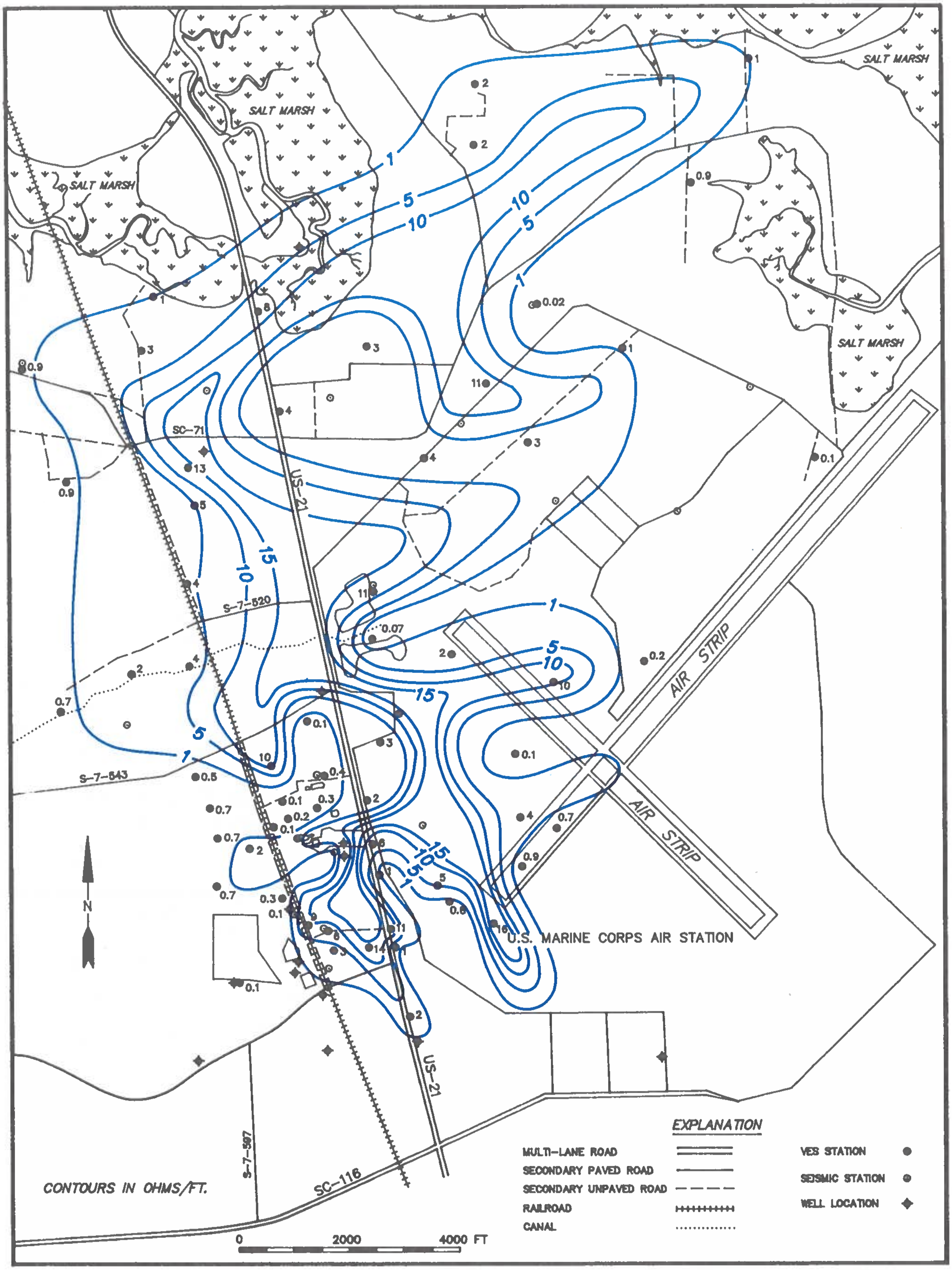

Figure 11. Contour map of true-resistivity values in the vinicity of the Burton recharge area.

the encroaching sea. The Beaufort Arch was a prominent feature that was inundated by the sea. As it was a topographic high, however, the deposits on this feature tend to be of a more shallow-water origin than those of the surrounding area. As the sea began to retreat, the area in the vicinity of the Beaufort Arch was emerging and shallow-water facies prevailed. As sea level continued to drop, upper shoreface deposits migrated over the Hawthorn clay and tidal channels, and inlets eroded underlying sediments. It appears that this was the time of erosion of the Hawthorn Formation, as evidenced on all the geologic sections (Plates 1-3). It appears that the Ocala Limestone was also partially eroded at this time (Fig. 12). Following the -60 foot contour on Figure 12, the shape tends to be long and narrow, suggesting that erosion was caused by channeling. Resistivity, well-log, and borehole data suggest that the channels were filled with sand. The 10-5 ohm/fit countour area (Fig. 10) and the 10-15 ohm/ft contour area (Fig. 11) appear to constrict to the south and south, forming multiple lobes. The constriction and the lobate shape of the contours suggest that the channel was terminating into an open body of water and the mouth of the tidal channel was being reworked into the lobate shape that is preserved today. In contrast, these coutours broaden to the northeast and spread out over a wide area, suggesting that the channel and associated depositional facies were located in a quiet lowland topography. On the basis of the geometry of these contours (Figs. 10-12) and data from wells and borings and surface geophysics, it is concluded that the Burton recharge area was formed by tidal channels eroding the Hawthorn Formation and partially scouring the upper part of the Ocala Limestone. The tidal channels appear to originate in the north and northeast portions of the study area and terminate in a tidal delta to the southeast.

Depositional Model

As stated above, the Burton recharge area was inundated by a transgressing sea during Pleistocene time. It appears that, because the study area was adjacent to the Beaufort Arch, sedimentation occurred predominantly in shallow water — most likely no deeper than lower shoreface. The sea also retreated to the south-southwest, as indicated by trifurcation of the channel (Figs. 10 and 11) followed by termination, suggesting the channels were approaching open water and formed a tidal delta in deep water. The tidal channels appear to have originated in the east-northeast portion of the study area, flowing south-southwest.

The east-northeast portion of the area was a quiet back-barrier lagoon or lowland marsh with tidal channels migrating back and forth across the lagoon or marsh. The migrating channels eroded the Hawthorn clay and partially incised the underlying limestone. It appears that the back-barrier area consisted mostly of sand-sized material rather than fine-grained sediments such as clay and silt, which is unusual for a back-barrier environment. Portions of the present-day back-barrier system along the South Carolina coast, however, are also sand dominated instead of mud dominated. Wojotal's (1981) study of the back-barrier system behind Kiawah Island (S.C.) found that the back-barrier environment consisted of a thin veneer of clay and silt ($\sim$60 cm) overlying very fine- to fine-grained sand. The primary source of sediments in the back-barrier/marsh behind Kiawah Island is the erosion of relic barrier sand ridges that consist mostly of sand, with very little clay and silt. It appears that the same situation occurred during Pleistocene deposition in the vicinity of the Beaufort Arch. The only exception is the sand that overlies the limestone, which had its source mainly in nearshore sands rather than upper shoreface barrier deposits. Therefore, as the migrating channels eroded the Hawthorn clay and incised the limestone, they deposited sand instead of back-barrier clay. Some back-barrier clay is still present in the study area. Data from BH-1 (Fig. 9) shows a dark-gray clay, approximately 8 inches thick, between the limestone and overlying sand. This has been interpreted as back barrier and not Hawthorn. In summary, the depositional model for the Burton recharge area is a sand-dominated back-barrier to upper shoreface environment that occurred during a marine regression in Pleistocene time.

Effect of Depositional Environment on Ground Water Movement

The movement of ground water in the subsurface is dependent on the hydraulic gradient and transmissivity — the latter being a function of hydraulic conductivity and aquifer thickness. In a large area, such as a county or group of counties, the effect of depositional environment on ground water movement is minor. On a smaller scale, however, such as the Burton recharge area, the effects of depositional environment are important in understanding the movement of ground water both vertically and horizontally. The flow of ground water is similar to the flow of electricity — both will seek the path of least resistance.

In order for the underlying aquifer to obtain significant recharge in the study area, the Hawthorn clay has to be absent. It appears that the areas where the clay is absent are also the areas where tidal channels have removed not only the Hawthorn clay, but also the upper portion of the limestone, and replaced the clay and limestone with

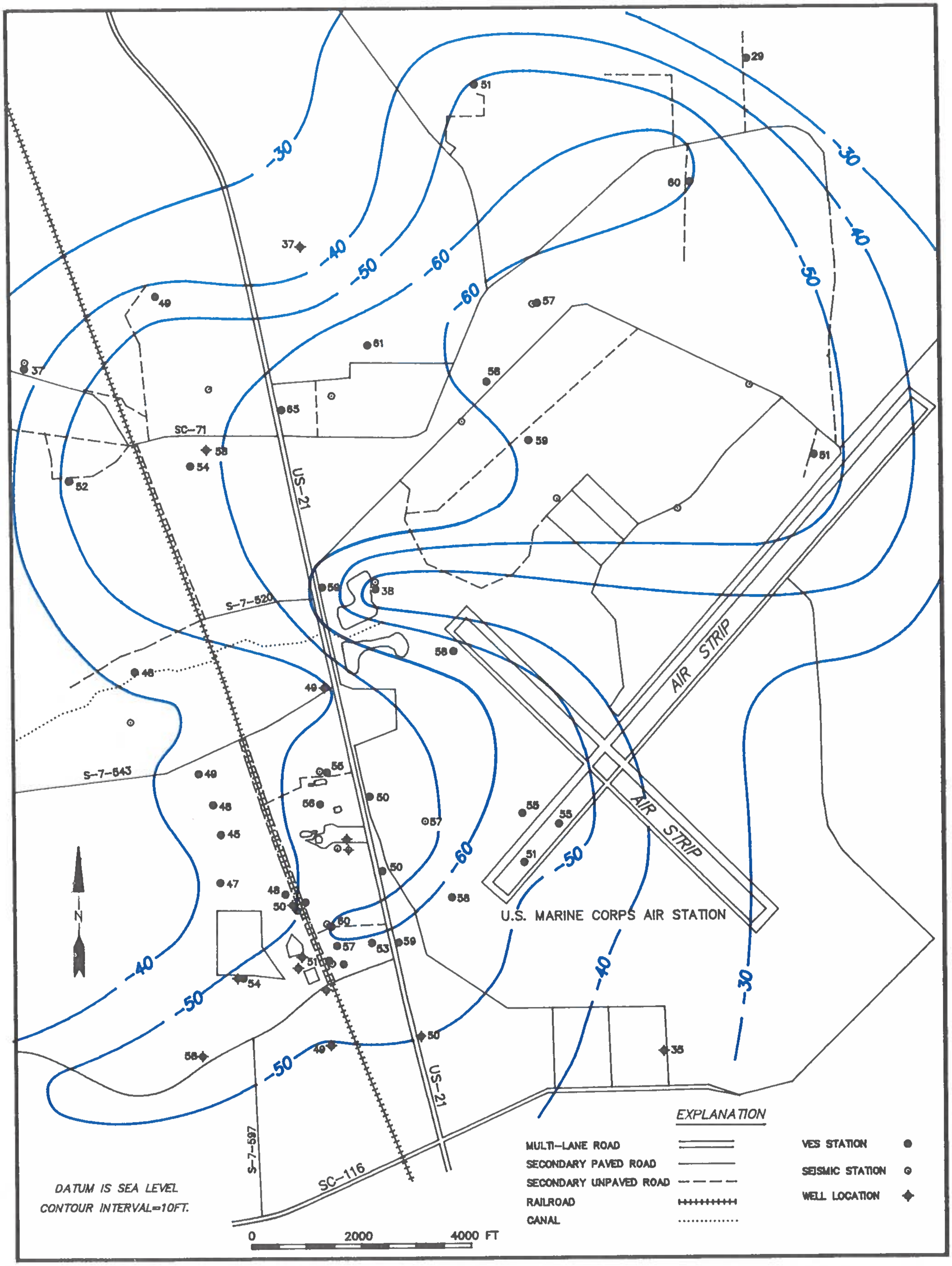

Figure 12. Stucture-contour map of the top of the Ocala Limestone in the vinicity of the Burton recharge area.

a medium- to fine-grained sand. With removal of the clay and deposition of sand, the upper shallow-water aquifer system now has a pathway to the limestone, allowing recharge to occur.

CONCLUSIONS

The depositional history of the sediments forming the shallow aquifer has been influenced by the presence of the Beaufort Arch and by fluctuations in sea level during the Pleistocene. The Beaufort Arch was a structural high during Pleistocene deposition, providing a shallow-water environment during high and low stands of sea level. Resistivity soundings and well and borehole data indicate that the absence of the confining unit separating the shallow-water aquifer from the artesian limestone is determined by the depositional history of the overlying sediments of the shallow aquifer. The Burton recharge area appears to have been created by tidal channels eroding the Hawthorn Formation during a low stand of sea level in Pleistocene time. The areas where the greatest amount of recharge might occur are those where not only the Hawthorn has been removed but also a portion of the underlying limestone.

Surface resistivity data for the study area were influenced primarily by water quality changes and iron precipitants coating the framework grains, rather than textural changes in the shallow-water aquifer system. Therefore, it is necessary to supplement the geophysical surveys with well and test boring data and not rely entirely on surface geophysics.

ACKNOWLEDGMENTS

I would like to thank the South Carolina Water Resources Commission and the South Carolina Coastal Council for providing funds for this study. Special thanks are due the staff in the Beaufort office of the SCWRC, particularly Mike Dale and A. D. Park, who assisted me in the field. I would also like to thank Jim Dorman and Jeff Cogan for their assistance in the field. Finally, I am grateful to the Commanding Officer and the Environmental Officer at the U.S. Marine Corps Air Station, Beaufort, for allowing access to the base for part of this study.

REFERENCES CITED

Benson, R. C., Glaccum, R. A., and Noel, M. R., 1982, Geophysical techniques for sensing buried wastes and waste migration: U.S. Environmental Protection Agency, Environmental Monitoring System Laboratory Report, p. 91-117.

Colquhoun, D. J., 1969, Geomorphology of the lower Coastal Plain of South Carolina: South Carolina Geological Survey Report MS-15, 36 p.

Colquhoun, D. J., 1971, Glacio-eustatic sea level fluctuation of the middle and lower Coastal Plain, South Carolina: Quaternaria, no. 15, p. 19-34.

Comer, C. D., 1968, Upper Tertiary stratigraphy of the lower Coastal Plain of South Carolina: Unpublished thesis, University of South Carolina, 17 p.

Cooke, C. W., 1936, Geology of the Coastal Plain of South Carolina: U.S. Geological Survey Bulletin 867, 189 p.

Dobrin, M. B., 1976, Introduction to geophysical prospecting (3rd edition): New York, McGraw-Hill, 630 p.

Haeni, F. P., 1984, Application of seismic-refraction techniques to hydrologic studies: U.S. Geological Survey Open-File Report 84-746, 144 p.

Hassen, J. A., 1985, Ground-water conditions in the Ladies and St. Helena Islands area, South Carolina: South Carolina Water Resources Commission Report 147, 44 p.

Hayes, L. R., 1979, The ground-water resources of Beaufort, Colleton, Hampton, and Jasper Counties, South Carolina: South Carolina Water Resources Commission Report 9, 84 p.

Heron, S. D., Jr., and Johnson, H. S., Jr., 1966, Clay mineralogy, stratigraphy, and structural setting of the Hawthorn Formation, Coosawatchie District, South Carolina: Southeastern Geology, v. 7, no. 2, p. 51-63.

Maher, J. C., 1971, Geologic framework and petroleum potential of the Atlantic Coastal Plain and Continental Shelf: U.S. Geological Survey Professional Paper 659, 98 p.

Minning, R. C., 1973, The electrical resistivity method — Technical memo number 3, part 1: Water Well Journal, v. 26, no. 6, p. 7-21.

Siple, G. E.,1960, Geology and ground-water conditions in the Beaufort area, South Carolina: U.S. Geological Survey Open-File Report, 124 p.

Spigner, B. C., and Ransom, C., 1979, Report on ground-water conditions in the Low Country area, South Carolina: South Carolina Water Resources Commission Report 132, 135 p.

Van Nostrand, R. G., and Cook, K. L., 1966, Interpretation of resistivity data: U.S. Geological Survey Professional Paper 499, 51 p.
Wojotal, A. M., 1981, Back-barrier stratigraphy of Kiawah Island, South Carolina: Unpublished dissertation, University of South Carolina.
Zohdy, A. A. R., Eaton, G. P., and Maybey, B. R., 1974, Application of surface geophysics to ground-water investigations — Chapter D1 in: Techniques of water-resources investigations of the United States Geological Survey: U.S. Geological Survey, Collection of Environmental Data, Book 2, p. 1-116.

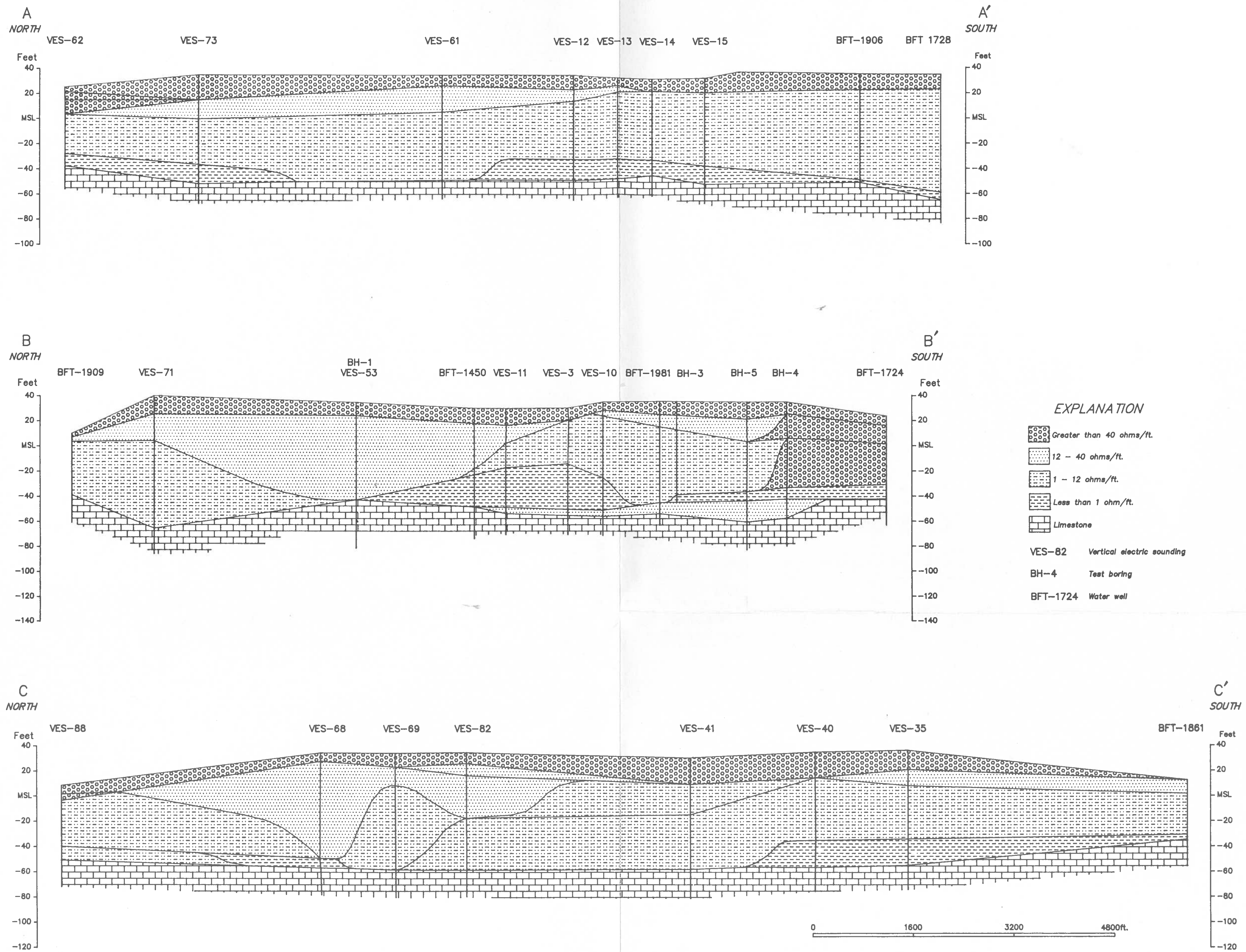

NORTH–SOUTH GEOELECTRIC SECTIONS IN THE VICINITY OF THE BEAUFORT HIGH

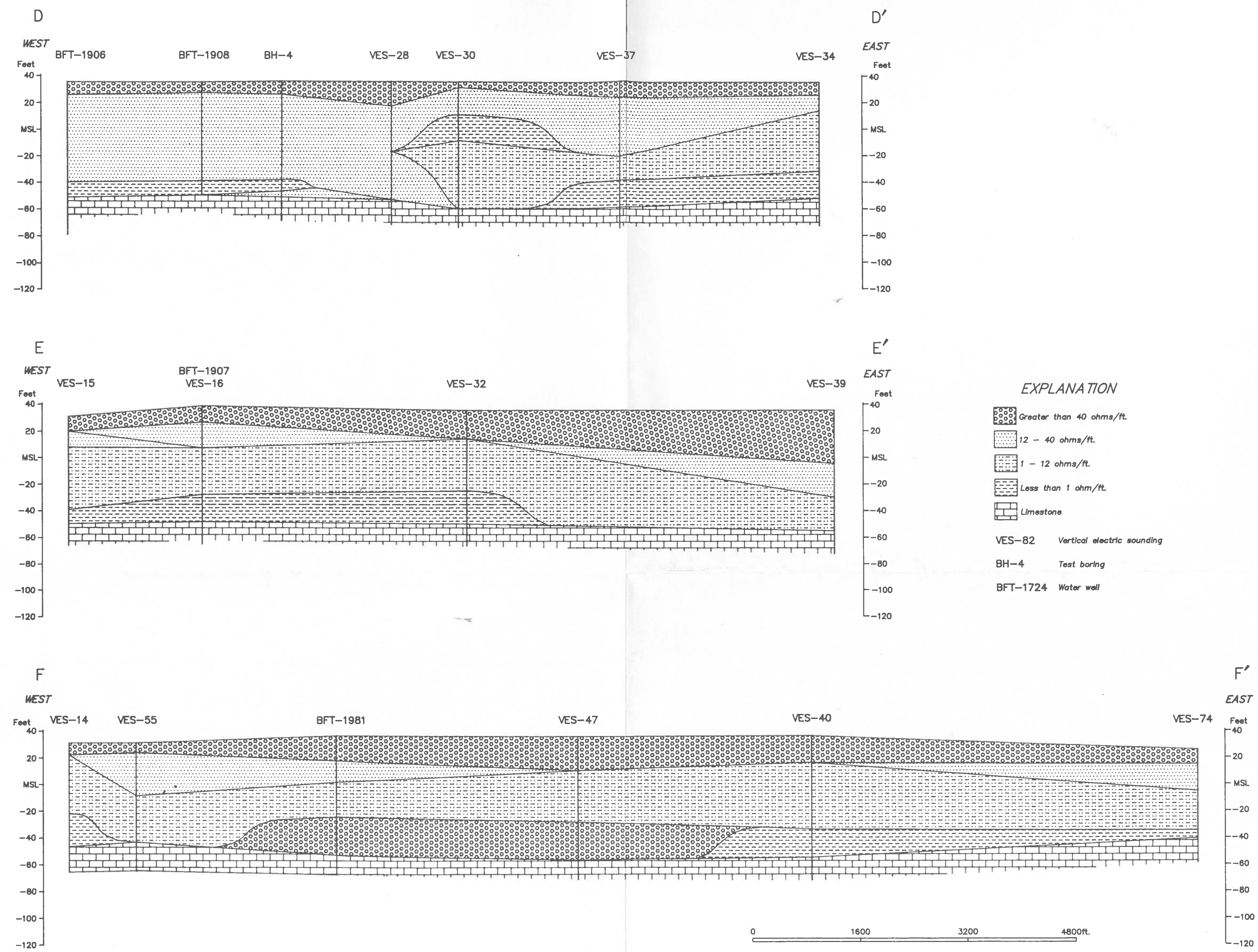

EAST–WEST GEOELECTRIC SECTIONS IN THE SOUTHERN PORTION OF THE BEAUFORT HIGH

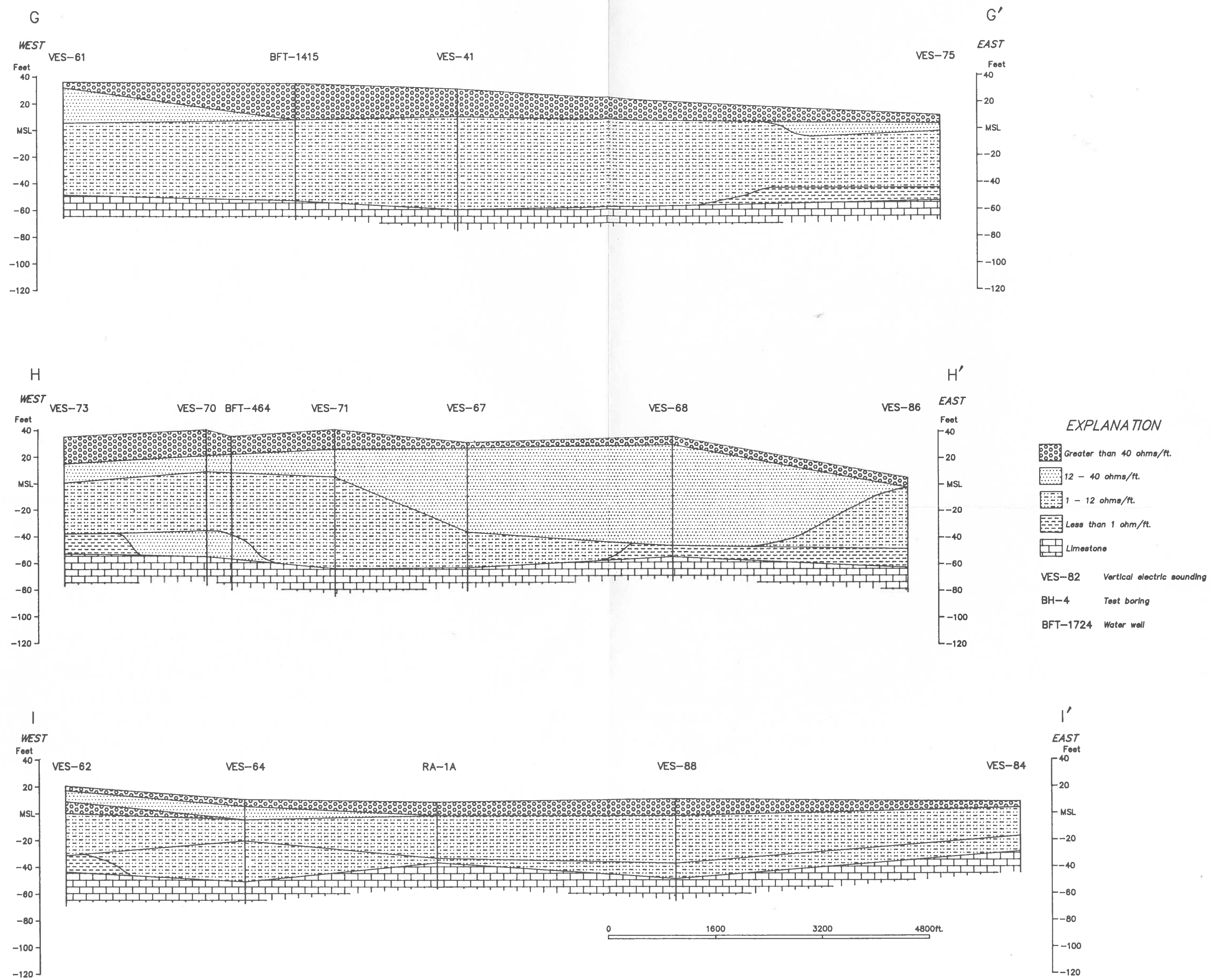

EAST-WEST GEOELECTRIC SECTIONS IN THE NORTHERN PORTION OF THE BEAUFORT HIGH